Journal Pre-proof

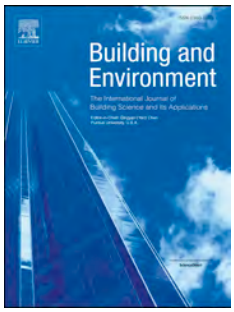

Evaluating a commercially available in-duct bipolar ionization device for pollutant removal and potential byproduct formation

Yicheng Zeng, Prashik Manwatkar, Aurélie Laguerre, Marina Beke, Insung Kang, Akram Ali, Delphine Farmer, Elliott Gall, Mohammad Heidarinejad, Brent Stephens

PII: S0360-1323(21)00158-X

DOI: https://doi.org/10.1016/j.buildenv.2021.107750

Reference: BAE 107750

To appear in: *Building and Environment*

Received Date: 17 December 2020

Revised Date: 22 February 2021

Accepted Date: 23 February 2021

Please cite this article as: Zeng Y, Manwatkar P, Laguerre Auré, Beke M, Kang I, Ali A, Farmer D, Gall E, Heidarinejad M, Stephens B, Evaluating a commercially available in-duct bipolar ionization device for pollutant removal and potential byproduct formation, *Building and Environment* (2021), doi: https://doi.org/10.1016/j.buildenv.2021.107750.

This is a PDF file of an article that has undergone enhancements after acceptance, such as the addition of a cover page and metadata, and formatting for readability, but it is not yet the definitive version of record. This version will undergo additional copyediting, typesetting and review before it is published in its final form, but we are providing this version to give early visibility of the article. Please note that, during the production process, errors may be discovered which could affect the content, and all legal disclaimers that apply to the journal pertain.

© 2021 Published by Elsevier Ltd.

Journal Pre-proof

Evaluating a commercially available in-duct bipolar ionization device for pollutant removal and potential byproduct formation

Yicheng Zeng[1], Prashik Manwatkar[1], Aurélie Laguerre[2], Marina Beke[1], Insung Kang[1], Akram Ali[1], Delphine Farmer[3], Elliott Gall[2], Mohammad Heidarinejad[1], and Brent Stephens[1]*

[1] Department of Civil, Architectural, and Environmental Engineering, Illinois Institute of Technology, Chicago, IL USA
[2] Department of Mechanical and Materials Engineering, Portland State University, Portland, OR USA
[3] Department of Chemistry, Colorado State University, Fort Collins, CO USA

*Corresponding Author:
Brent Stephens, PhD
Professor and Department Chair
Department of Civil, Architectural, and Environmental Engineering
Illinois Institute of Technology
Alumni Hall Room 228E
3201 S Dearborn Street
Chicago, IL 60616 USA

Keywords: indoor air quality, air cleaner, ionizer, particulate matter, volatile organic compounds

Abstract

We conducted a series of experiments to evaluate the gas and particle removal effectiveness and potential for byproduct formation resulting from the operation of a commercially available in-duct bipolar ionization device. Laboratory tests were conducted with the ionizer installed in a small air handler serving a large semi-furnished chamber. Chamber experiments were conducted under (i) normal operating conditions to characterize the impact of the ionizer on particle concentrations (0.01-10 µm), ozone (O_3), nitrogen dioxide (NO_2), volatile organic compounds (VOCs), and aldehydes, and (ii) particle injection and decay conditions to characterize the impact of the ionizer operation on particle loss rates. The field test involved air sampling of particulate matter (0.01-10 µm), O_3, and VOCs upstream and downstream of an operating ionizer device installed in an air handling unit serving an occupied office building. Both the chamber and field tests suggested that the use of the tested bipolar ionization unit led to a

Journal Pre-proof

decrease in some hydrocarbons (e.g., xylenes) among the lists of compounds we were able to target, but an increase in others, most prominently oxygenated VOCs (e.g., acetone, ethanol) and toluene. Ionizer operation appeared to minimally impact particle, O_3, and NO_2 concentrations during normal operating conditions. Particle injection and decay experiments in the chamber suggest that operation of the ionizer unit led to a small increase in loss rates for ultrafine particles (<0.15 µm) and a small decrease in loss rates for larger particles (>0.3 µm), but with negligible net changes in estimated $PM_{2.5}$ loss rates.

1. Introduction

As a result of recent global air quality challenges, including smoke from historically large wildfires in the U.S. (Xu et al., 2020) and the increasing recognition of the potential for aerosol transmission of COVID-19 in poorly ventilated indoor environments (CDC, 2020a), there has been an unprecedented level of interest and investment in indoor air cleaning technologies. The marketplace for air cleaning devices has become inundated with an array of technologies to meet the demand, including high-efficiency fibrous-media filters, disinfectant misters, and a variety of electronic air cleaners including ultraviolet germicidal irradiation (UVGI) lights, plasma generators, hydroxyl radical generators, ionizers, and more (Elejalde-Ruize, 2020; Environmental and Modelling Group (EMG), 2020; Johnson Controls, 2020; Mandavilli, 2020; Ori, 2020). While fibrous media filters are routinely tested for their ability to remove particles (ASHRAE, 2017; ISO, 2016), many electronic air cleaning technologies are not evaluated by any federal agency or industry standards organizations for their efficacy or their potential for unintended consequences, including the generation of chemical byproducts (US EPA, 2018).

One such air cleaning technology that has garnered significant interest is air ionization, which involves the introduction of ions to a space. Air ionization devices include those that generate only negative ions (i.e., *unipolar* ionizers) and those that generate both positive and negative

ions (i.e., *bipolar* ionizers). Air ionization has been shown in some peer-reviewed studies to decrease bacterial deposition to surfaces (Meschke et al., 2009), inactivate airborne bacteria (Hyun et al., 2017; Nunayon et al., 2019), remove airborne particles (Pushpawela et al., 2017), and increase submicron particle deposition to surfaces (Wu et al., 2015). While the efficacy for some of these constituents has been demonstrated in some peer-reviewed studies, the literature remains sparse and limited to a narrow range of technologies.

More commonly, efficacy is demonstrated in test reports provided by commercial laboratories, although these tests commonly have limitations such as multiple ionizers in small (or unreported) volume test chambers or with high (or unreported) ion concentrations. Moreover, the potential for byproduct formation resulting from ionizer operation has been investigated in much less depth. Early tests on ionizer devices revealed the potential to form harmful byproducts such as ozone during operation (Zhang et al., 2011), but manufacturers have since developed other forms of ionization technologies that have been shown to avoid ozone emissions (Nunayon et al., 2019). However, a limited number of other studies have shown the potential for ionization to form other products, including nitrogen oxides (NO_x) and VOC oxidation intermediates (Kim et al., 2017), although little peer-reviewed literature exists on byproduct formation in either laboratory or field settings.

Two recent studies evaluated the impacts of air ionization on markers of human health. One study investigated the short-term effects of a negative ion generating air purifier on cardiovascular and respiratory outcomes in healthy adults in Beijing (Liu et al., 2020). The study concluded that exposure to negative ions (~60,000 ions/cm^3) was associated with increased systemic oxidative stress levels (a biomarker of cardiovascular health), and even though the use of the ionizers decreased indoor particulate matter concentrations, as intended, there were no beneficial changes in other markers of respiratory health. This phenomenon was hypothesized

to be due to byproducts formed from reactions with negative ions, although byproducts were not measured. Another recent study found similar outcomes in 11-14 year old children resulting from the use of air ionizers in school classrooms in Beijing, whereby some positive effects on respiratory health were measured at elevated ion concentrations of ~13,000 #/cm^3, albeit at the expense of negative effects on cardiac health (Dong et al., 2019). These studies demonstrate the potential for air ionization to be effective in reducing particulate matter, but also the potential for ionization to generate potentially harmful byproducts during their operation.

The most widely used ionization approach currently in the U.S. appears to be *bipolar ionization*, which is commonly reported to (i) reduce airborne particulate matter by causing them to cluster or agglomerate and form larger particles that can settle out of the air more rapidly or be filtered more effectively, (ii) neutralize odors and break down volatile organic compounds (VOCs), (iii) inactivate or kill viruses and other microorganisms, and (iv) reduce the amount of required outdoor air. Many engineers have been recommending bipolar ionization devices because of relatively low upfront costs for purchase and installation, low maintenance and materials costs, and they do not introduce additional pressure drop to air handling units. In fact, the Building Owners and Managers Association (BOMA) currently recommends to “explore the possible use and efficacy of bi-polar ionization and other technology for the HVAC system that are effective against COVID” (BOMA, 2020).

Conversely, ASHRAE summarizes the literature on electronic air cleaners, including ionizers, in their Epidemic Task Force (ETF) Filtration and Disinfection Guidance, as well as in their most recent position document on filtration and air cleaning, as ranging from “ineffective” to “very effective” in reducing airborne particle concentrations (ASHRAE, 2020, 2018). ASHRAE’s COVID-19 resources also cite a statement from a representative from the US Centers for Disease Control and Prevention (CDC) that recommends consumers “request efficacy

Journal Pre-proof

performance data that quantitatively demonstrates a clear protective benefit under conditions consistent with those for which the consumer is intending to apply the technology" and that "the documented performance data under as-used conditions should be available from multiple sources, some of which should be independent, third party sources." Recent guidance from the CDC considers ionization and other air disinfection technologies as "emerging" technologies "in the absence of an established body of peer-reviewed evidence showing proven efficacy and safety under as-used conditions" (CDC, 2020b). We are not aware of investigations of the effectiveness or potential for byproduct formation of bipolar ionization devices used in realistic settings, which presents a knowledge gap that this work intends to fill.

2. Methods

We conducted a series of experiments to evaluate the gas and particle removal effectiveness and potential for byproduct formation resulting from the operation of a commercially available bipolar ionization device in two different test settings: one laboratory (large chamber) setting in Chicago, IL, USA and one field setting in a city in Eastern Oregon (OR) USA. The same make and model 'needlepoint' bipolar ionization device (Global Plasma Solutions, GPS-FC48-AC, Charlotte, NC USA) was tested in each location. We did not assess efficacy in inactivating microbes or potential pathogens.

2.1 Laboratory (Large Chamber) Experiments (Chicago, IL)

Because ions added to indoor environments can react with other compounds present in indoor air, potentially leading to the formation of intermediates and oxidation byproducts, we conducted a series of experiments in a large (36.7 m^3) aluminum environmental chamber recently constructed on the main campus of Illinois Institute of Technology in Chicago, IL USA (Figure 1). The chamber is located in a large laboratory space and was not directly heated or cooled, but was served by a small custom-built air-handling unit supplying air from the surrounding

Journal Pre-proof

conditioned laboratory space. Laboratory air was pulled through a charcoal fiber filter (Hydrofarm IGSCFF4, Petaluma, CA USA) on the return side and ducted into the chamber via a flexible aluminum duct. The air handler and ductwork were operated in a single pass-through mode to provide approximately 40-120 m^3/h, depending on the fan speed setting, of moderately filtered air from outside the chamber into the chamber without any recirculation. The surrounding laboratory space was minimally occupied by researchers during testing.

A variety of (mostly aged) material emission sources were introduced into the chamber prior to testing to simulate a partially furnished office or similar environment with a variety of relatively constant VOC emission sources that introduce a 'challenge' indoor VOC mixture with which ions generated by the tested ionizer would conceivably interact. Materials introduced to the chamber included a used table, rug, plastic and metal chairs, suit jackets, scarf, window shades, paper posters, foam packaging materials, multiple boxes of dissertations ranging in publication date from the 1960s to 1990s, and used painting tray, and more. Several dissertations were also left open on the table to encourage emissions. Transient VOC emission sources were specifically avoided in order to ensure reasonably steady-state conditions could be achieved. A small fan was placed in the corner of the chamber to encourage mixing throughout testing. A CO_2 injection and decay test with three CO_2 monitors (calibrated via co-location tests) located in three different locations within the chamber confirmed reasonably well-mixed conditions (Figure S1).

A single GPS-FC48-AC bipolar ionization unit was installed inside the small air-handling unit serving the chamber, positioned upstream of the fan in a small custom-fabricated return plenum. The ionizer was secured to the bottom surface of the return plenum and connected to a 120 VAC power source. The on/off switch for the device extended to the outside of the air handler to allow for powering on the ionizer without disrupting airflow conditions. The manufacturer data

sheet for the GPS-FC48-AC unit states that it is designed to accommodate airflows from 0 to 4,800 ft^3/min (~8,155 m^3/h) and generates >400 million ions/cc/sec (GPS, 2019).

The goal of this test setup was to deliver ions into the chamber space at an ion concentration that followed our understanding of manufacturer recommendations as closely as possible and at an air change rate with the surrounding environment that was (i) similar to that commonly observed in offices and other commercial buildings (e.g., 1-1.5 air changes per hour (Bennett et al., 2012; Persily and Gorfain, 2004)) and that also (ii) allowed for reasonably rapid approaches to steady-state conditions for air sampling and for comparisons of pollutant concentrations between ionizer off and on conditions. Air change rates with the surrounding lab air were measured periodically inside the chamber using CO_2 injection and decay to ensure these conditions were met. Repeated CO_2 injection and decay experiments before and after testing confirmed a typical chamber air change rate with air from the surrounding lab area of ~1.2-1.6 per hour (1/h). The system was a single pass system without recirculation.

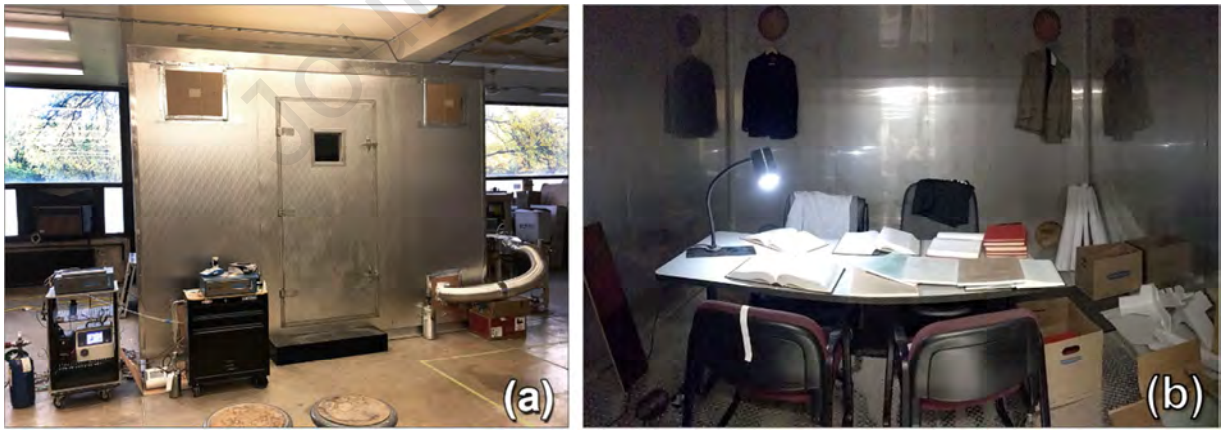

Figure 1. Photos of the environmental test chamber: (a) exterior with instruments set up outside and (b) inside of the chamber with mock-up furnishings and materials.

Initial measurements of total volatile organic compound (TVOC) concentrations inside and outside the chamber, both before and after introducing furnishing and materials, were made using a ppbRAE 3000 photoionization detector (PID) monitor (RAE Systems, San Jose, CA

USA), which confirmed that the introduction of furnishings and materials led to an increase in TVOC concentrations (as isobutylene equivalents) inside the chamber compared to background conditions and that approximately steady-state conditions could be reached within ~3 hours (Figure S2). Additionally, measurements of ion concentrations were made periodically inside and outside the chamber, both with and without the ionizer operating, using an AlphaLab Air Ion Counter (Gerdien Tube meter) prior to testing (AlphaLab, Inc., Salt Lake City, UT USA). Background ion concentrations inside the laboratory (outside the chamber) and inside the chamber typically ranged between ~300 and ~700 ions/cm^3. Operation of the ionizer increased ion concentrations inside the chamber to steady-state concentrations of ~1400 to ~2000 ions/cm^3, which is consistent with the manufacturer recommended target of 1500-2000 ions/cm^3 in spaces in which they are installed (Direct Supply, 2020), albeit lower than ~13,000 ions/cm^3 and ~60,000 ions/cm^3 reported in the recent studies of short-term health outcomes associated with using a different type of ionizer as previously mentioned (Dong et al., 2019; Liu et al., 2020) and much lower than the high concentrations (i.e., >10^6 ions/cm^3) that have been associated with lower depression scores (Perez et al., 2013). While this installation and setup is not the same as a real-life installation in an occupied building, we have confidence that the resulting combination of ion concentrations, ventilation conditions, and, to an extent, indoor VOC concentrations, reasonably represent conditions of a typical unoccupied indoor space with this ionization unit installed in the air handler serving the space.

Once the chamber, air handler, and ionizer were set up, a series of experiments were conducted over multiple test days to evaluate the gas and particle removal effectiveness and potential for byproduct formation resulting from ionizer operation. The experimental design was intended to capture the effects of ionizer operation under (i) normal operating conditions and (ii) particle injection and decay conditions.

Journal Pre-proof

2.1.1 Normal operating conditions

First, a series of experiments were conducted under normal operating conditions (i.e., without any particle or pollutant injection other than from the supplied laboratory air and the materials and furnishings inside the chamber) to measure a variety of constituents inside and outside the chamber with the air handler operating, once with the ionizer powered on and once with the ionizer powered off. We repeated the same normal condition experiments on multiple days under similar conditions, once on October 15, 2020 to primarily focus on measurements of VOCs inside and outside of the chamber (which required sampling and offline analysis at a commercial laboratory), followed by another test day on October 24, 2020 to focus on measurements of particles, ozone, and nitrogen oxides inside and outside of the chamber.

During these experiments, we measured the following constituents inside and/or outside the chamber: (i) airborne particles using a TSI Model 3910 NanoScan Scanning Mobility Particle Sizer (SMPS; ~0.01-0.4 µm; TSI Shoreview, MN USA) and a TSI Model 3330 Optical Particle Sizer (OPS; 0.3-10 µm), (ii) ozone (O_3) using a 2B Technologies Model 211 ozone analyzer (2B Technologies, Boulder, CO USA), (iii) nitrogen oxides (NO_x) using a 2B Technologies Model 405 NO_x analyzer, and (iv) CO_2 using Extech SD800 CO_2 monitors located inside and outside the chamber (Extech, Nashua, NH USA). After the October 15, 2020 test day, the particulate matter and NO_x sampling instruments were each connected to automated switching valves (Swagelok Model SS-43GXS4-42DCX electrically actuated three-way ball valves; one each for PM and NO_x; Swagelok, Solon, OH USA) to alternately measure concentrations inside and outside the chamber at 20-minute intervals throughout the duration of testing (Zhao et al., 2019; Zhao and Stephens, 2017, 2016). The switching valve was controlled automatically by an electronic timer (Sestos B3S-2R-24; Hong Kong). The O_3 instrument was not connected to a switching valve.

Journal Pre-proof

On the October 15, 2020 sampling day conducted to characterize gas-phase organics, we sampled for (i) VOCs using SUMMA canisters (Entech 1.4L Silonite Coated stainless steel Minicans with a flow restrictor providing approximately 30 minute fill duration), with off-line analysis conducted via EPA method TO-15 as well as a NIST library compound search to tentatively identify compounds not on the TO-15 list, and (ii) aldehydes and carbonyls following EPA method TO-11A using 2,4-Dinitrophenylhydrazine (DNPH) sampling tubes connected to sampling pumps (Buck Libra Model L-4) with off-line analysis conducted via high-performance liquid chromatography (HPLC). Off-line chemical analysis was conducted at a commercial laboratory (STAT Analysis, Chicago, IL), as described in more detail later in this section. Sampling pump flow rates for TO-11A sampling were confirmed after sampling to be ~1.6-1.7 L/min prior to sampling using a Sensidyne Gilian Gilibrator-2 bubble flow meter (Sensidyne, St. Petersburg, FL USA). Time-integrated VOC and aldehyde samples were collected using the SUMMA canisters and DNPH tubes, respectively, beginning at least two hours after perturbation of the chamber (i.e., both before and after the ionizer was switched on) such that the chamber should have approached steady-state conditions by the time of sampling. All sampling devices (except for one CO_2 monitor) were located outside the chamber with sampling lines running into the chamber through openings approximately 0.36 m off the floor, which were sealed with cardboard and tape. Particle instruments were connected to rigid stainless steel sampling lines ~1.5 m in length and ~0.5 cm in diameter via TSI conductive tubing; O_3, NO_x, and SUMMA canisters were connected to flexible polytetrafluoroethylene (PTFE) tubing for sampling. Temperature and relative humidity were measured continuously both inside and outside the chamber using a combination of Onset HOBO U12-012 (Onset, Bourne, MA USA) and Extech SD800 CO_2 monitors.

The timeline of the normal operating condition experiments on the single VOC sampling day (October 15, 2020) is shown in Figure 2. The air handling unit serving the chamber was turned

on around 9:45 am local time, with the ionizer off for the first several hours of measurements. The chamber operated at this condition for nearly 3 hours to allow for approaching steady-state baseline conditions inside the chamber. VOCs were then sampled inside and outside the chamber during these baseline (ionizer off) conditions beginning around 12:30 pm. The SUMMA canister valves were opened for approximately 30 minutes and the DNPH samplers were operated from about 12:30 pm to 2:57 pm for inside sampling and 1:10 pm to 2:57 pm for outside sampling. After VOC sampling with the ionizer off was completed, the ionizer was turned on at 3:16 pm. The ionizer remained on for the duration of the rest of the tests. After approximately two hours of operating the system, around 5:16 pm, we again began sampling for VOCs and aldehydes inside and outside the chamber using new SUMMA canisters and DNPH tubes, respectively. Again, the SUMMA canister valves were opened for approximately 30 minutes and the DNPH personal air sampling pumps were operated with new DNPH tubes from ~5:16 pm until ~7:45 pm. A blank DNPH tube was placed outside the chamber throughout testing to serve as our blank control sample. Finally, CO_2 injection and decay was conducted around 7:45 pm to measure the air change rate in the chamber.

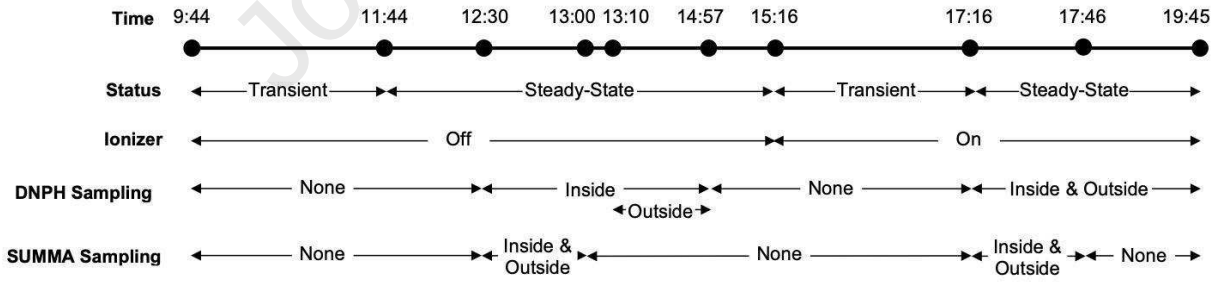

Figure 2. Timeline of the VOC sampling day experiments conducted during normal operating conditions (October 15, 2020).

After sampling, the DNPH cartridges and field blanks were individually capped and wrapped in aluminum foil and kept in a refrigerator held at ~4°C. The following day, a total of five DNPH tubes (placed in a thermally insulated box) and four SUMMA canisters were returned to a commercial laboratory for chemical analysis (STAT Analysis, Chicago, IL), including two inside

Journal Pre-proof

chamber samples (one with ionizer off; one with ionizer on); two outside chamber samples (one with ionizer off; one with ionizer on); and one blank. STAT Analysis originally supplied the evacuated SUMMA canisters for VOC sampling and DNPH cartridges for aldehyde sampling. The SUMMA canisters were analyzed via a purge and trap volatile autosampler on an Agilent 6890 gas chromatograph (GC) with an Agilent 5973 mass selective detector (MS). This results in a chromatogram that shows mass spectral data for any detected compound as well as retention time. The commercial laboratory has a calibrated list of compounds that it can quantitate against. The MS also allowed for an assessment of tentatively identified compounds (TICs), which have peaks and spectrum show up in the chromatogram, but are not a part of the calibrated list. These TICs were reported from comparing the MS data to a known NIST library of compounds; library compound search reports were provided by the lab for subsequent analysis. DNPH cartridges were also acquired from the same commercial laboratory and returned for analysis, which involved extraction in solvent and analysis on an Agilent 1100 HPLC system against a list of known compounds from the TO-11A list. Concentrations from DNPH sampling were calculated by dividing mass values provided by STAT Analysis by the volume of the sample (calculated as the pump flow rate times the sample time). STAT Analysis calibrates their analytical systems to the list of compounds in TO-15 and TO-11A; the TICS allow for some semi-quantitative assessment of additional TICs not in these lists. Full lists of compounds from the TO-15 and TO-11A analysis are provided in Appendix 1 and Appendix 2. Method blanks were included with each run and verified that target compounds were below reporting limits (RL).

On the October 24, 2020 sampling day, which was designed to characterize impacts on particulate matter, O_3, and NO_x during normal operating conditions, all instruments were set to log data at 1-min intervals. To analyze the resulting measurements of particulate matter and NO_x concentrations from the instruments connected to automated switching valves, we noted

the time that initial sampling began with the automated valves sampling from inside the chamber, and then flagged the data points in each 20-minute sampling interval as either inside or outside the chamber in alternating fashion. Transition points between inside and outside sampling periods were identified visually in the data and excluded from analysis. Ratios of the concentrations of constituents inside and outside of the chamber (i.e., I/O ratios) were calculated using summary statistics (mean, standard deviation) from each 20-minute interval of inside chamber sampling, lagged by the previous 20-minute interval of outside chamber sampling.

2.1.2 Particle injection and decay

After conducting experiments during normal operating conditions, a series of particle injection and decay experiments were conducted to explore the impact of ionizer operation on particle decay rates in the chamber. These experiments were conducted on two separate days: one day with the ionizer operating (October 31, 2020) and one day without the ionizer operating (November 8, 2020). The chamber was maintained at approximately the same airflow and environmental conditions for both days of testing, which were also similar to the normal operating condition experiments. Particles were generated by burning two sticks of incense placed on a shelf on the desk inside of the chamber. Incense sticks were allowed to burn to completion to avoid researcher entry into the chamber, extinguishing after approximately 30 minutes, and then particle concentrations were allowed to decay for 2-4 hours under each test condition.

Measurements of particle concentrations during these experiments were made again using a TSI NanoScan SMPS and TSI OPS to measure particle number concentrations in size ranges from ~0.01 μm to ~10 μm at 1-minute intervals, again connected to the sampling system with an electronically controlled automated switching valve, alternating between 20-minute periods

Journal Pre-proof

sampling inside the chamber and 20-minute periods sampling outside the chamber. CO_2 was also injected into the chamber at the same time as incense burning to simultaneously measure the air change rate with the surrounding lab.

2.1.3 Data analysis and parameter estimation

Particle injection and decay data were first visually explored on a size-resolved basis (up to 13 bins for SMPS and up to 16 bins for OPS). For simplicity in making comparisons, integral measures total particle number concentrations measured by each instrument were used in the analysis. The Nanoscan SMPS has known issues with counting efficiencies, especially in size ranges > 0.15 µm, during some conditions due to the method used to fit distributions required because of the use of a unipolar charger in the instrument (Yamada et al., 2015; Zhao and Stephens, 2017). Total number concentrations measured by each instrument (SMPS and OPS, respectively) -- were calculated at each 1-minute measurement interval as the sum of the concentrations measured in each size bin measured by each instrument (i.e., 0.01-0.15 µm for the SMPS and 0.3-10 µm for the OPS). Additionally, integral measures of $PM_{2.5}$ mass concentrations were estimated at each time interval by calculating the mass concentration in each size bin smaller than 2.5 µm from combination of the SMPS and OPS, assuming spherical shape and constant unit density m (Cheng et al., 1995; Ji et al., 2010). However, we acknowledge that the assumption of unit density may result in an underestimate of $PM_{2.5}$ mass (Patel et al., 2020).

We used a dynamic mass balance approach to model the time-varying inside particle concentration for all SMPS and OPS size bins in the well-mixed chamber after the incense sticks extinguished (i.e., in the absence of indoor particle sources), as shown in following Equation 1.

$$\frac{dC_{in}}{dt} = P\lambda C_{out} - (\lambda + k)C_{in} \quad (1)$$

where *P* is penetration factor (-), λ is the air change rate of the chamber (1/hr), *k* is the particle deposition loss rate constant (1/hr), C_{out} and C_{in} are the outside and inside particle concentrations at time *t*, respectively (#/cm^3 or #/m^3).

To solve for the total particle loss rate constant (λ + *k*), we used a first-order linear regression solution to the natural logarithm of the particle concentration data measured inside the chamber minus that measured inside the chamber during background conditions applied only to the decay period, as shown in Equation 2.

$$-ln\frac{C_{in,t}-C_{bg}}{C_{in,t=0}-C_{bg}} = (\lambda + k)t \quad (2)$$

where $C_{in,t}$ and $C_{in,t=0}$are the inside particle concentrations at time *t* and *t=0*, respectively. C_{bg} is the average particle concentration measured inside the chamber during approximately steady-state conditions either immediately prior to or after the particle injection and decay periods.

For each test using CO_2 as a tracer gas, the air change rate (λ) was estimated by regressing the natural logarithm of the inside and outside CO_2 concentrations versus time, as shown in Equation 3.

$$-ln\frac{Y_{in,t}-Y_{out}}{Y_{in,t=0}-Y_{out}} = \lambda t \quad (3)$$

where $Y_{in,t}$ and $Y_{in,t=0}$ are the CO_2 concentrations (ppm) measured inside the chamber at time *t* and *t*=0, respectively. Y_{out} is the average CO_2 concentration (ppm) measured outside the chamber using a second monitor during the test period. The two CO_2 monitors had been previously calibrated to each other via co-location tests.

2.2 Field Measurements (Oregon, USA)

A separate set of measurements were made at a field site in Oregon, USA with an operating needlepoint bipolar ionization system (again, GPS-FC48-AC) installed in the air handling unit (AHU). The study site was a 360 m^2 office building that was occupied during the measurements. Between five and eight people were present for the duration of monitoring, and two other individuals also entered the space for short durations. The building was served by two AHUs and an ionizer unit was installed into both air handlers. We conducted sampling upstream and downstream of the ionizer unit in the AHU that served a conference room, two offices, a restroom, and an archive room, consisting of ~178 m^2 of floor area. The supply duct was approximately 0.61 m x 0.53 m and the design supply air flow rate was 1,000 ft^3/min (1,700 m^3/h).

We conducted air sampling in four locations in the building: 1) ~0.75 m upstream the ionizer unit in the supply duct, 2) ~0.75 m downstream the ionizer unit in the supply duct (Figure 3), 3) in the outdoor air supply duct, and 4) inside an 11.5 m^2 office served by the AHU where upstream and downstream sampling occurred. At each location, we measured particulate matter, size-resolved in 27 bins between 0.01 µm and 10 µm using a TSI Model 3910 Nanoscan SMPS and a TSI Model 3330 OPS, O_3 using a 2B Technologies Model 106-OEM-L, and VOCs sampled onto AirToxic glass sorbent tubes (Perkin Elmer), packed with 180mg of Carbotrap B followed by 70 mg of Carboxen 1000, and analyzed by thermal desorption–gas chromatography–mass spectrometry (TD-GC-MS). Details regarding the TD-GC-MS method are provided in Appendix 3. In all locations except the location downstream of the ionizer, temperature and relative humidity were measured continuously (Onset, S-THB-M002).

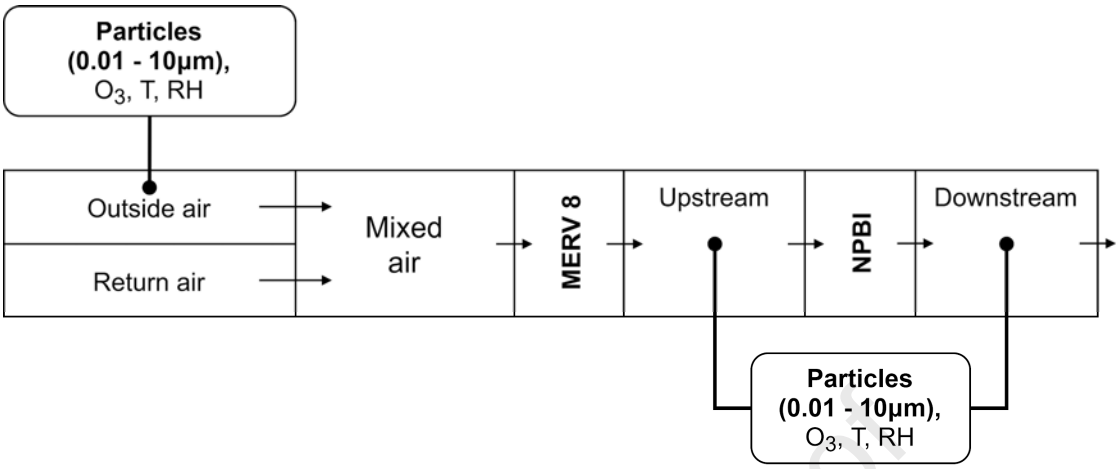

Figure 3. Schematic of the AHU in the field site with sampling locations marked. Arrows indicate the direction of airflow through the AHU. MERV = Minimum efficiency reporting value, NPBI^{TM} = needlepoint bipolar ionizer, O_3 = ozone, T = temperature, RH = relative humidity.

The ionizer unit in the field location was turned on at the beginning of the workday, ~8:00 am local time, with measurements beginning at approximately 11:30 am local time. The ionizer remained on for the duration of the tests. For measurements made in the supply duct, we measured air pollutant concentrations over a 1 h period. For particle measurements, we sampled air upstream and downstream of the ionizer through two runs of ~1.5 m of ⅜" conductive tubing (bev-a-line) that was installed through a sampling port drilled into the aluminum duct. Every five minutes, we manually switched the line attached to the instruments from the upstream to downstream (or vice versa), recording the timestamp of the switch in a laboratory notebook. For ozone, we similarly sampled from air upstream and downstream the ionizer through two runs of ~1.5 m of ¼" perfluoroalkoxy (PFA) tubing, switching every five minutes manually. Upstream of the ionizer system, we inserted the temperature and relative humidity (RH) probe into the center of the supply air duct. Particles, ozone, temperature, and RH were all recorded in a 1-min interval. VOC measurements were time-integrated in each location upstream and downstream the ionizer, with two sampling pumps drawing air through two runs of ~0.5 m of ⅛" diameter PFA tubing with a target flow rate of ~50 mL/min for each

pump. VOCs were sampled in duplicate at each location for 1 h, for a total sample volume of ~3 L in each sorbent cartridge. In outdoor air and inside the office, we sampled particles, ozone, temperature and RH, and VOCs in two 30-min sampling events occurring in series. VOC samples were made with single replicate during outdoor sampling and in duplicate during indoor air sampling.

We sampled in the supply duct upstream and downstream of the ionizer to isolate and observe immediate impacts of the ionization unit. Additional measurements made in the indoor space and outdoor space were made to compare supply, indoor, and outdoor concentrations. Note that we did not have capability to control the indoor space, including occupancy, behaviors, and activities. We also did not have access to the mechanical systems such that we could shut off the ionizer system; therefore, we do not have field data that include a control where the air handling system is operating but the ionization system is off.

3. Results

3.1 Laboratory (Large Chamber) Experiments (Chicago, IL)

In this section, we present data from the large chamber laboratory experiments in Chicago, first for the normal operating condition experiments, then followed by the particle injection and decay experiments. Table 1 summarizes the chamber test days and their measurement focus, and also provides average (standard deviation, SD) temperature and relative humidity values measured during each experiment, as well as the measured air change rate with the surrounding laboratory air. Air change rates of 1.2 to 1.6 per hour were achieved during the test periods approximately as intended, including ~1.25 per hour with the air handling unit set to low fan speed and ~1.59 per hour with the air handling unit set to medium fan speed.

Table 1. Large chamber test condition summary, with average temperature and RH inside and outside the chamber during each test condition

Date	Condition	Target	Sample Location	Temperature (°C) Mean (SD)	RH (%) Mean (SD)	Air Change Rate (1/hr)
Oct 15, 2020	Normal operation	VOCs	Inside	23.4 (1.2)	26.5 (4.4)	1.25
			Outside	24.2 (1.2)	25.0 (4.5)	
Oct 24, 2020	Normal operation	PM, O_3, NO_x	Inside	26.9 (2.7)	26.2 (1.3)	1.59
			Outside	23.9 (0.1)	25.6 (0.8)	
Oct 31, 2020	Injection & Decay	PM	Inside	24.3 (1.0)	29.8 (0.6)	1.26
			Outside	22.1 (0.7)	31.2 (1.3)	
Nov 8, 2020	Injection & Decay	PM	Inside	25.7 (0.3)	39.0 (1.7)	1.26
			Outside	24.3 (0.1)	48.4 (0.5)	

3.1.1 Normal operating condition experiments

This section summarizes particle concentrations, select VOC concentrations, O_3, and NO_x concentrations measured during the normal operating condition experiments conducted in the large chamber.

3.1.1.1 Particle concentrations

Figure 4 shows particle concentrations measured inside and outside the chamber on the October 24, 2020 test day under normal operating conditions with periods of ionizer on and off marked in time. Each data point represents a 1-minute interval reading, and readings alternate from 20-minute sampling periods inside followed by 20-minute sampling periods outside. Figure 4a shows total number concentrations measured by the SMPS (Total SMPS: ~0.01-0.3 µm); Figure 4b shows total number concentrations measured by the OPS (Total OPS: 0.3-10 µm); and Figure 4c shows estimates of $PM_{2.5}$ concentrations made using data from both the SMPS and OPS. Particle concentrations inside the chamber were lower than concentrations outside the chamber, but closely tracked outside chamber concentrations over time. There was a spike in OPS-measured and estimated $PM_{2.5}$ mass concentrations outside the chamber immediately prior to and immediately after switching on the ionizer, likely due to the movements and

activities of research personnel. Comparing ionizer on and off periods visually, there were no obvious periods of particle generation or removal inside the chamber for any of the particle measures.

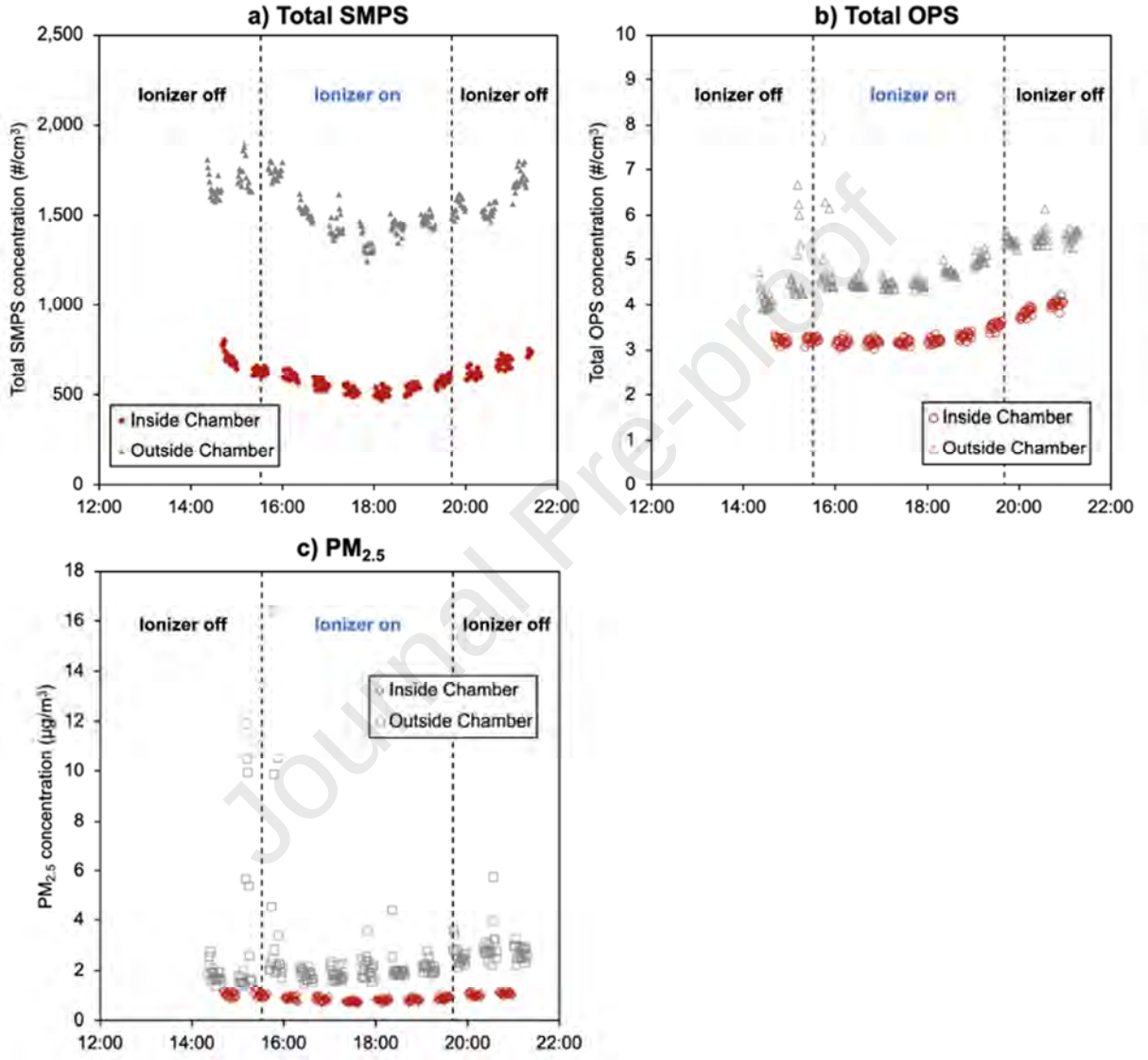

Figure 4. Particle concentrations measured inside and outside the chamber, alternating every 20 minutes, on the October 24, 2020 sampling day with the ionizer on and off periods marked: a) total number concentrations measured by the TSI NanoScan SMPS (~0.01-0.3 µm), b) total number concentrations measured by the TSI OPS (0.3-10 µm), and c) estimated $PM_{2.5}$ mass concentrations made using both the SMPS and OPS data.

Figure 5 shows inside/outside (I/O) chamber concentration ratios measured throughout the October 24, 2020 test day. I/O ratios are calculated for each of the three particle measures (total

SMPS, total OPS, and $PM_{2.5}$) using the mean inside chamber concentration in a given 20-minute sampling interval divided by the mean outside chamber concentration in the prior 20-minute interval. Uncertainty in I/O ratios at each 40-minute combined I/O sample interval is estimated by adding the relative standard deviations of the inside and outside concentrations at each interval in quadrature. I/O ratios are important to use for comparison purposes because Mann-Whitney U tests revealed significant differences in the absolute number concentrations of all particle measures (total SMPS, total OPS, and $PM_{2.5}$) measured outside the chamber between the ionizer on and off periods ($p<0.05$, Figure 4), as well as inside the chamber between the ionizer on and off periods ($p<0.05$, Figure 4). Normalizing inside chamber concentrations to outside chamber concentrations accounts for these variations over time that are likely unrelated to ionizer usage. Figure 5a shows I/O ratios for each 40-minute combined I/O sample interval over time, with periods of ionizer on and off marked in time. Figure 5b shows mean (SD) I/O ratios from the same data, grouped by ionizer on and off periods.

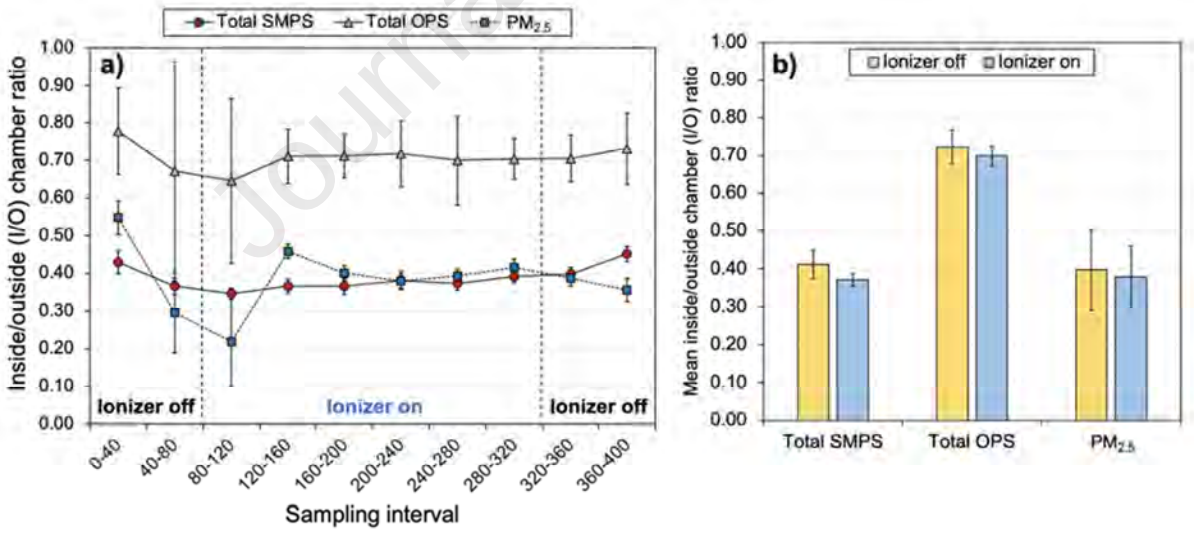

Figure 5. Inside/outside (I/O) chamber concentration ratios calculated for three particle measures (total SMPS, total OPS, and $PM_{2.5}$) on the October 24, 2020 sampling day under normal operating conditions with the ionizer on and off periods marked: a) I/O ratios for each 40-minute combined I/O sample interval over time, and b) mean (SD) I/O ratios, grouped by ionizer on and off periods. I/O ratios are calculated for each of the three particle measures using the mean inside chamber concentration in a given 20-minute sampling interval divided by the mean outside chamber concentration in the prior 20-minute interval. Uncertainty in I/O ratios at each 40-minute combined I/O sample interval is estimated by adding the relative standard deviations of the inside and outside concentrations at each interval in quadrature.

Large standard deviations in I/O ratios were apparent immediately before and after switching on the ionizer, driven by large fluctuations in particle concentrations (OPS, >0.3 µm) outside the chamber. Otherwise, I/O ratios were relatively steady throughout the test day with both the ionizer on and off. The mean (±SD) I/O ratio for the total SMPS concentrations was 0.41±0.04 with the ionizer off and 0.37±0.02 with the ionizer on (~10% decrease), but differences in these values were not statistically significant ($p = 0.09$, Mann-Whitney U test). The mean (±SD) I/O ratio for the total OPS concentrations was 0.72±0.05 with the ionizer off and 0.70±0.03 with the ionizer on (~3% decrease), but differences in these values were not statistically significant ($p = 0.39$, Mann-Whitney U test). The mean (±SD) I/O ratio for estimated $PM_{2.5}$ concentrations was 0.40±0.10 with the ionizer off and 0.38±0.08 with the ionizer on (~5% decrease), but differences in these values were also not statistically significant ($p = 0.67$, Mann-Whitney U test). These results suggest that while I/O ratios for each particle measure were slightly lower with the ionizer on than with the ionizer off, the differences were not statistically significant, and may have been affected by variations in concentrations outside the chamber during the test period. Note that the Mann-Whitney U tests applied to these data are underpowered, with small sample sizes of $n = 6$ intervals with the ionizer on and $n = 4$ intervals with the ionizer off.

3.1.1.2 VOC and aldehyde concentrations

Tables 2 and 3 show results for the detection and quantification of organic compounds on the VOC sampling day (October 15, 2020). Table 2 shows compounds identified and quantified using the TO-15 and TO-11A target list of compounds; confidence in both detection and quantification in Table 2 is high given the analytical laboratory's calibrations for these target analytes. Table 3 shows concentrations of organic analytes tentatively identified and pseudo-quantified in the library compound search of spectral peaks detected outside of the TO-15 target list from the SUMMA canister samples.

Table 2. Organic compound analysis for the TO-15 and TO-11A analyte lists applied to samples collected inside (I) and outside (O) the chamber during ionizer on and off conditions on October 15, 2020.

Test Method	Analyte	MW (g/mol)	Ionizer Off			Ionizer On			% Change in I/O Ratio[1]
			Inside (µg/m^3)	Outside (µg/m^3)	I/O Ratio	Inside (µg/m^3)	Outside (µg/m^3)	I/O Ratio	
TO-11A	Formaldehyde	30	11.4	5.9	1.95	10.6	5.3	1.98	+2%
TO-11A	Acetaldehyde	44	5.9	5.4	1.10	5.7	4.6	1.25	+13%
TO-15	Acetone	58	23	36	0.64	41	37	1.11	+73%
TO-11A	Butyraldehyde	72	2.1	2.0	1.06	2.2	1.6	1.35	+28%
TO-15	Toluene	92	2.6	4.5	0.58	3.4	5.1	0.67	+15%
TO-15	1,2-Dichloroethane	99	4.1	<2.4	>1.7	<2.4	<2.4	n/a	At least -42%
TO-15	Ethylbenzene	106	7.5	<2.7	>2.8	<2.7	<2.7	n/a	At least -64%
TO-15	m,p-Xylene	106	24	<5.2	>4.6	<5.2	<5.2	n/a	At least -78%
TO-15	Dichlorodifluoromethane	121	3.6	<3.0	>1.2	<3.0	<3.0	n/a	At least -17%
Total	Summed TOC[2]	n/a	84.2	58.9	1.43	68.0	58.8	1.16	-19%

[1] Inside/outside (I/O) chamber ratios are calculated for each ionizer on and off period. The % change in I/O ratio shows comparisons between all inside/outside (I/O) chamber values when possible. When an analyte was reduced inside the chamber below reporting limit (< RL) and/or when the outside chamber concentration of an analyte also found inside the chamber was < RL, then the % change in I/O ratio for that analyte was estimated to be "at least" the shown percent change.

[2] The summation of total organic compounds (TOC) is the sum of the concentrations of each of the analytes shown for each sample. The I/O ratio for summed TOC is calculated as the summed TOC value for inside chamber values divided by the summed TOC value for outside chamber values for each of the ionizer on and off conditions.

Table 2 reveals several key observations regarding air composition inside and outside the chamber during testing. First, the summation of total organic compounds (TOC) from the combination of TO-15 and TO-11A analyses shows that summed VOC concentrations were higher in the chamber (84 µg/m^3) than outside of the chamber (59 µg/m^3) during baseline (ionizer off) conditions (i.e., an I/O chamber ratio of ~1.4). Present in the indoor challenge mixture in the greatest amounts were: m,p-Xylene (~24 µg/m^3), acetone (~23 µg/m^3), and formaldehyde (~11 µg/m^3). These compounds and their magnitudes are reasonably consistent with medians and means observed in the US EPA Building Assessment Survey and Evaluation Study (BASE) study of office buildings (US EPA, n.d.) and in a recent study of a variety of commercial retail buildings in California (Chan et al., 2015). Second, summed TOC values for these targeted analytes in Table 2 were similar outside the chamber during both ionizer on and off conditions (~59 µg/m^3), suggesting reasonably constant conditions during testing in the lab area surrounding the chamber.

Third, summed TOC values for these targeted TO-15 and TO-11A analytes were lower during the ionizer on period than the ionizer off period, with summed TOC concentrations inside chamber decreasing from 84 µg/m^3 to 68 µg/m^3 (19% decrease in I/O chamber ratio). However, the ionizer operation appeared to lead to varying responses for individual compounds, with some increasing in concentration and others decreasing. For example, concentrations of higher molecular weight compounds (>95 g/mol) 1,2-dichloroethane, ethylbenzene, m,p-xylene, and dichlorodifluoromethane were each reduced from above detection limits prior to ionization to below detection limits during ionization, with percent reductions in I/O chamber ratios ranging from at least 17% to >78% for these compounds. Conversely, concentrations of some of the lower molecular weight compounds identified in the TO-15 and TO-11A analyte lists increased during ionizer operation, including acetone with a ~73% increase in I/O ratio (and from 23 µg/m^3 to 41 µg/m^3 inside the chamber with fairly constant concentrations outside the chamber), butyraldehyde (i.e., butanal) with a ~28% increase in I/O ratio (with some potential attribution to variations in concentrations outside the chamber), and toluene with a ~15% increase in I/O ratio (from 2.6 µg/m^3 to 3.4 µg/m^3 inside the chamber).

These data suggest that while ionization led to a decrease in some hydrocarbons, the ionization process appears to have led to partial decomposition of some hydrocarbons, resulting in the observed increases in some oxygenated VOCs. This proposed phenomenon of incomplete VOC degradation is consistent with the ionization process charging VOCs, and then those VOC ions (VOC+ or VOC-, depending on ionization mechanism) either decomposing to a smaller VOC and an accompanying ion, or going on to react with molecular oxygen (O_2). The resulting ion-molecule cluster (e.g., [VOC•O2]+) could then undergo a rearrangement to form a carbonyl group (C=O), producing the observed enhancements in some oxygenated VOCs (oVOCs).

Some of the carbonyl-containing compounds did not increase, but that may be a function of analytical detection limits and the original concentration of precursors to form those aldehydes. The observed increase in toluene from use of the ionizer was unexpected, as toluene is an oxygen-free hydrocarbon, but we hypothesize that it is a decomposition or fragmentation product following ionization of larger aromatics. Further, the net formation of acetone provides further insight on potential VOC degradation - and oVOC production - mechanisms. Acetone has an ionization energy (IE) of 9.7 eV, so ambient acetone should be ionized in the bipolar ionization device. However, the net formation of acetone indicates that it is also being produced, either as a decomposition product of other, larger ketones, or as an oxidation product following the charged VOC+ ions binding with O_2 and undergoing subsequent rearrangement and/or decomposition reactions.

Table 3 further demonstrates some compound-specific effects of the ionizer operation, albeit with much less certainty in identification and quantification than the TO-15 and TO-11A results in Table 2 because of high uncertainties in the TICS process. Quality values from the NIST library compound search are reported in Table 3 and should be interpreted as general indicators of quality that primarily serve to distinguish between highly uncertain identification (i.e., lower quality values <20) and more certain identification (i.e., higher quality values >50). Several tentatively identified compounds were detected only in outside chamber samples and not inside chamber samples with both low and high quality values. Ethanol was detected in all samples and appeared to lead to an increase in I/O chamber ratios of more than 50%, with inside chamber concentrations remaining fairly constant during both ionizer on and off periods, while outside chamber concentrations decreased during ionizer operation.

Table 3. Organic compound analysis for analytes tentatively identified in a compound search (TICS) of the GC-MS analysis of SUMMA canister samples collected inside (I) and outside (O) the chamber during ionizer on and off conditions on October 15, 2020. (ND = not detected).

			Ionizer Off			Ionizer On			% Change in I/O Ratio[1]
Test Method	Tentatively Identified Analyte (Quality)	MW (g/mol)	Inside ($\mu g/m^3$)	Outside ($\mu g/m^3$)	I/O Ratio	Inside ($\mu g/m^3$)	Outside ($\mu g/m^3$)	I/O Ratio	
TICS	Acetonitrile (<10)	44	ND	6	<< 1	ND	17.3	<< 1	n/a
TICS	Ethanol (<10 ionizer off; >50 ionizer on)	46	13.8	15.9	0.87	12.8	8.3	1.54	+78%
TICS	3-Butenamide (10)	85	ND	ND	n/a	1.9	ND	> 1	↑
TICS	4-Penten-1-ol (27)	86	ND	1.8	< 1	ND	ND	n/a	n/a
TICS	Hexanal (40)	100	ND	2.1	< 1	ND	2.5	n/a	n/a
TICS	Hexane, 3,3-dimethyl- (64)	114	3.8	ND	> 1	2.5	ND	> 1	↓
TICS	Hexane, 2,3,5-trimethyl- (50)	128	2.8	ND	> 1	ND	ND	n/a	↓
TICS	1R-.alpha.-Pinene (76)	136	ND	2.2	< 1	ND	ND	n/a	n/a
TICS	Cyclohexene, 4-ethenyl-1,4-dimethyl (50)	136	ND	ND	n/a	1.9	ND	> 1	n/a
TICS	3-Phenyl-1-butanol (<10)	150	2	ND	> 1	ND	ND	n/a	↓
TICS	Nonane, 4,5-dimethyl (64)	156	1.8	ND	> 1	ND	ND	n/a	↓
TICS	Decane, 4-ethyl- (59)	170	ND	ND	n/a	9.2	ND	>> 1	↑
TICS	Undecane, 4,6-dimethyl- (72)	184	ND	ND	n/a	5.7	ND	>> 1	↑
TICS	Undetermined[2] (<10)	und.	ND	ND	n/a	17.9	ND	>> 1	↑
Total	Summed TOC	-	24.2	28.0	0.86	51.9	28.1	1.85	+114%

[1] Inside/outside (I/O) chamber ratios are calculated for each ionizer on and off period. The % change in I/O ratio shows comparisons between all inside/outside (I/O) chamber values when possible. Given the uncertainties in both identification and quantification of the compounds from the TICS, the % change in I/O ratios is shown for only a limited number of constituents, and otherwise shows qualitative increases or decreases with an up or down arrow.
[2] Tentatively identified compound possibilities include: ethylene oxide (44 g/mol; quality <10), carbon dioxide (44 g/mol; quality <10), octodrine (129 g/mol; quality <10), or 2-Heptanamine, 5-methyl- (129 g/mol; quality <10).

Several tentatively identified compounds with higher identification confidence (i.e., quality >50) were reduced from some level of identification and quantification to no identification or quantification during ionizer operation, including potentially 3,3-dimethyl-Hexane, 2,3,5-trimethyl-Hexane, and 4,5-dimethyl-Nonane, each with likely identified MW > 100 g/mol. Conversely, several tentatively identified compounds were detected during ionizer operation that were not originally identified without ionizer operation, including potentially 3-Butenamide (small increase, low quality), 4-ethenyl-1,4-dimethyl-Cyclohexene (small increase, moderate quality), 4-ethyl-Decane (larger increase, higher quality), and 4,6-dimethyl-Undecane (larger increase, higher quality), each with MW > 80 g/mol. There was also an increase in an indeterminable

compound, with mass spectral peaks at either 44 g/mol or 129 g/mol, that could not be identified with high enough quality to yield further insight. While these TICS comparisons should be interpreted with caution (i.e., tentative in identification and even less confidence in quantification), these results further support findings in Table 2 of varied responses in individual compounds in the chamber presumably due to the ionization process, including some being detected or increasing only with the ionizer on and some only with the ionizer off.

3.1.1.3 O_3 and NO_2 concentrations

Figure 6 shows O_3 and NO_2 concentrations measured inside the chamber during one of the normal operating condition experiments with and without the ionizer operating, conducted on October 24, 2020. Concentrations of both constituents inside the chamber were low (i.e., median of ~1.5-2 ppb for O_3 and ~4 ppb for NO_2) both with and without the ionizer operating, as is fairly typical for an indoor environment with no known sources of either constituent (Salonen et al., 2019; Xu et al., 2017; Zhou et al., 2019) and with moderate gas-phase filtration on the air intake. There were no significant differences (i.e., neither an increase nor a decrease) in NO_2 concentrations measured inside the chamber with or without the ionizer operating (Mann-Whitney U-test $p=0.29$). There was a small, statistically significant decrease in O_3 concentrations inside the chamber with the ionizer operating compared to ionizer off conditions (Mann-Whitney U-test $p<0.05$), with median values of ~2 ppb and ~1.5 ppb, respectively. However, this difference was well within instrument uncertainty and O_3 concentrations outside the chamber were not measured but could have varied as well. Operation of the ionizer as described in the chamber clearly did not generate detectable O_3 or NO_2 emissions, nor did it appear to substantially decrease concentrations of either O_3 or NO_2 at these low concentrations. A time-series of O_3 concentration in the chamber is shown in Figure S3, which illustrates this small decrease, as well as a lack of detectable O_3 emissions. Our finding of no O_3 emissions is

consistent with publicly available reports of standardized testing of this same technology using UL Standards 867 and 2998.

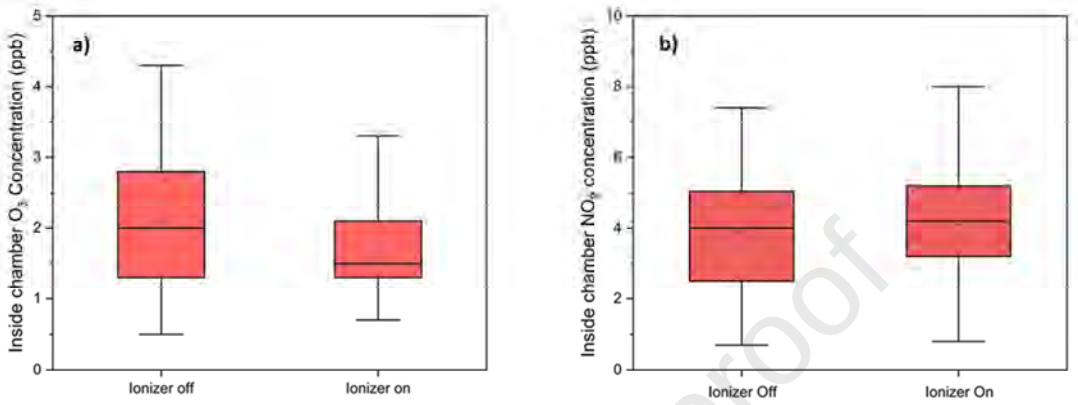

Figure 6. Concentrations of (a) O_3 and (b) NO_2 measured inside the chamber during the normal operating condition experiment with the ionizer on and off on October 24, 2020.

3.1.2 Particle injection and decay experiments

This section details results from the particle injection and decay experiments conducted on October 31, 2020 (with the ionizer on) and November 8, 2020 (with the ionizer off). Figure 7 shows profiles of integral measures of particle number concentrations (i.e., total SMPS for particle sizes ~0.01-0.15 µm and total OPS for particle sizes 0.3-10 µm) during the entire injection and decay process. Burning of incense in the chamber increased total particle concentrations in the 0.01-0.15 µm size range from less than 10,000 #/cm^3 during baseline conditions to ~160,000 #/cm^3 at peak concentrations, and subsequently decayed back to baseline values over time. Similarly, burning of incense in the chamber increased total particle concentrations in the 0.3-10 µm size range from less than 200 #/cm^3 during baseline conditions to ~2,500 #/cm^3 at peak concentrations, and also subsequently decayed back to baseline values over time. There were no major differences in the injection and decay process with the ionizer on or off conditions, although the ionizer off test period was shorter than the ionizer on period. The estimated $PM_{2.5}$ concentrations averaged ~4-5 µg/m^3 during baseline conditions on

both test days and peaked between ~750 and ~900 µg/m^3 during the height of the injection period. Figure S4 shows results from air change rate measurements using CO_2 injection and decay made during the particle injection and decay experiments conducted on October 31, 2020 (with the ionizer on) and November 8, 2020 (with the ionizer off). On both days, the air change rate with the surrounding space was estimated to be ~1.26 1/h, demonstrating the ability to achieve consistent chamber test conditions on different days of experiments.

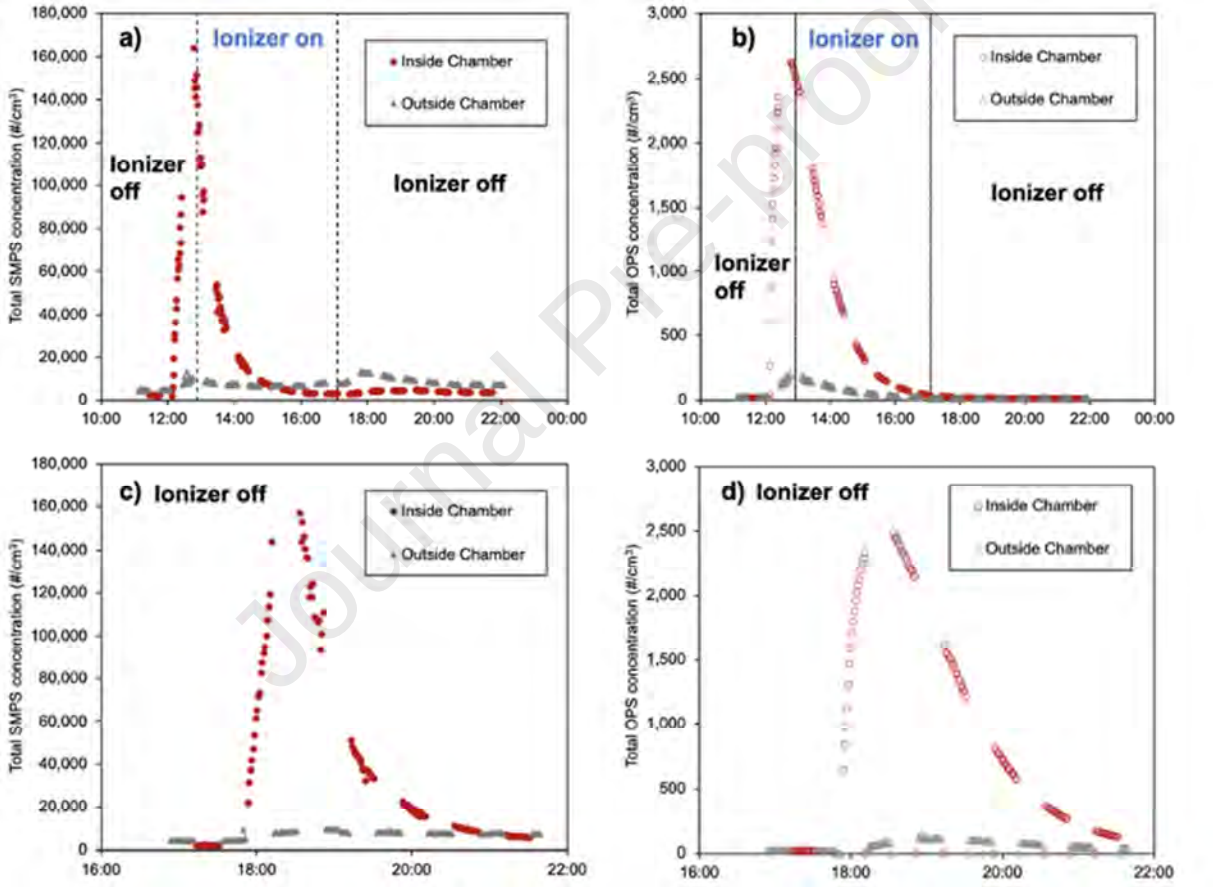

Figure 7. Time-series profiles of total particle concentrations measured by the SMPS (0.01-0.15 µm) and OPS (0.3-10 µm) during particle injection and decay experiments: (a) total SMPS and (b) total OPS on the ionizer test day (October 31, 2020), and (c) total SMPS and (d) total OPS on the test day without the ionizer operating (November 8, 2020). Vertical dashed line in (a) and (b) demonstrate when the ionizer was switched on and off.

Figure 8 shows estimated total particle loss rates ($\lambda + k$) resulting from the particle injection and decay experiments conducted on October 31, 2020 (with the ionizer on) and November 8, 2020

(with the ionizer off) for three integral particle measures of (a) $PM_{2.5}$, (b) total number concentrations in the 0.01-0.15 µm size range measured by the SMPS (i.e., "Total SMPS"), and (c) total number concentrations in the 0.3-10 µm size range measured by the OPS (i.e., "Total OPS"). Deposition loss rate constants (k) can be estimated by subtracting the air change rate (λ) from the total loss rate ($\lambda + k$), although since the air change rate was the same in each condition, total loss rates can be used for direct comparison between ionizer on and off conditions.

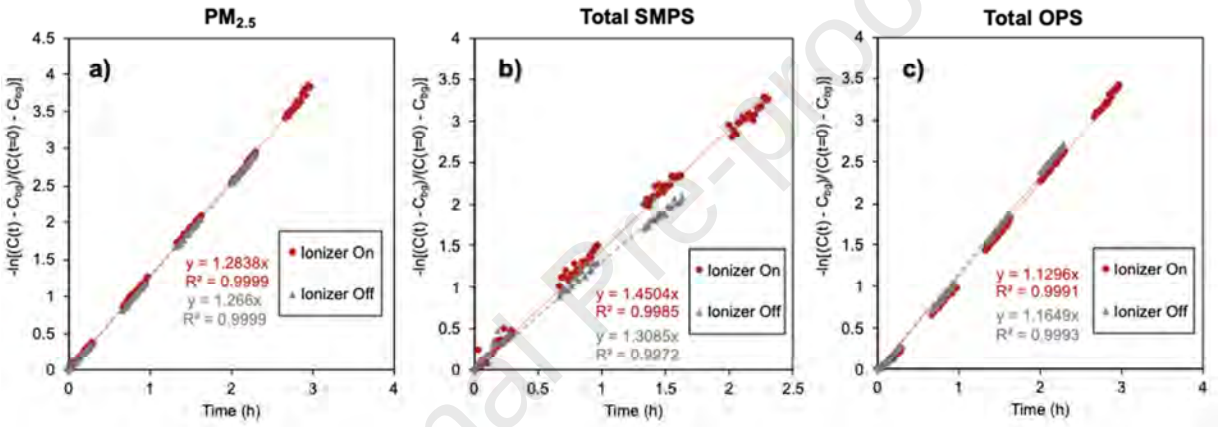

Figure 8. First-order loss rate constants ($\lambda + k$) with the ionizer on and off for the following: (a) $PM_{2.5}$ mass concentrations, (b) total number concentrations measured by the SMPS (0.01-0.15 µm), and (c) total number concentrations measured by the OPS (0.3-10 µm). Chamber air change rates were measured to be ~1.26 1/h on both test days.

Figure 8a demonstrates that the operation of the ionizer did not meaningfully increase $PM_{2.5}$ loss rates in the chamber, as loss rates were ~1.27 1/h with the ionizer off and ~1.28 1/h with the ionizer on. The difference of ~0.01 1/h (<1%) between ionizer on and off conditions is within the uncertainty of the regression approach. Figure 8b demonstrates that the loss rates of the integral measure of total particles 0.01-0.15 µm measured by the SMPS apparently increased from ~1.31 1/h with the ionizer off to ~1.45 1/h with the ionizer on (an increase in total SMPS loss rates of ~11%). Conversely, Figure 8c demonstrates that the operation of the loss rates of the integral measure of total particles 0.3-10 µm measured by the OPS apparently decreased from ~1.16 1/h with the ionizer off to ~1.13 1/h with the ionizer on (a small decrease in total OPS

Journal Pre-proof

loss rates of ~3%). For reference, multiplying these differences in loss rates by the volume of the chamber yields equivalent clean air delivery rate (CADRs) in this test configuration of approximately 0.7 m^3/h (0.4 cfm), 5.2 m^3/h (3 cfm), and -1.3 m^3/h (-0.8 cfm) for $PM_{2.5}$, Total SMPS, and Total OPS particulate matter metrics.

These results suggest that although the operation of the ionizer appeared to have led to some differences in particle loss rates between the ultrafine (i.e., 0.1-0.15 µm measured by the SMPS) and fine and coarse (0.3-10 µm measured by the OPS) size ranges, the net impacts on estimates of total $PM_{2.5}$ loss rates were negligible. This observation of an increase in loss rates for ultrafine particles (<0.15 µm), a decrease in loss rates for larger particles (>0.3 µm), and no net change in $PM_{2.5}$ loss rates is conceivably explained in a way that could be consistent with agglomeration of small particles into larger particles, as smaller particles could have grown out of the <0.15 µm size range (thus increasing loss rates in the range) but then appeared in the >0.3 µm size range (thus decreasing loss rates in the range), yet did not grow large enough to encourage more rapid deposition to surfaces in the test chamber. In other words, while these results suggest that the reported mechanism of action of the ionizer (agglomeration or particle growth) may be working, particle mass was still conserved and the ionizer function contributed to shifting the size distribution slightly in the direction of larger particles.

3.2. Field Measurements (Oregon, USA)

Figure 9 shows monitoring results for particle size distributions (Figure 9a), total particle number concentration from 0.01-10 µm (Figure 9b), and ozone concentrations (Figure 9c) measured in the four locations in the office building described in Section 2.2. Particle number and size distributions upstream and downstream of the ionization unit are similar; it does not appear that particle agglomeration occurred over the short length (~0.75 m) from the ionizer to the downstream sampling location in the supply duct. This finding is not unexpected, given the short

residence time in the duct from the upstream to downstream sampling location. However, if an ionization system is installed with the intent to increase the single-pass particle removal efficiency of a filter (Park et al., 2011; Shi and Ekberg, 2015) by agglomeration, agglomeration would need to occur within the time-scale of transport from the ionizer to the filter. Data shown in Figure 9 demonstrate that particle size distributions are not substantially altered in the timeframe of transport from the ionization unit to the downstream sampling location. Further testing is warranted, e.g., following ASHRAE Standard 52.2, to determine the impacts of upstream ionization on mechanical filtration particle removal efficiency. We observe an increase in particles >1 micrometer in indoor air compared to measurements made downstream of the ionizer, though we cannot discern whether this effect is due to the ionization unit or the presence of occupants in the indoor space. We also observed similar ozone concentrations upstream and downstream of the ionizer, implying the system is not generating ozone.

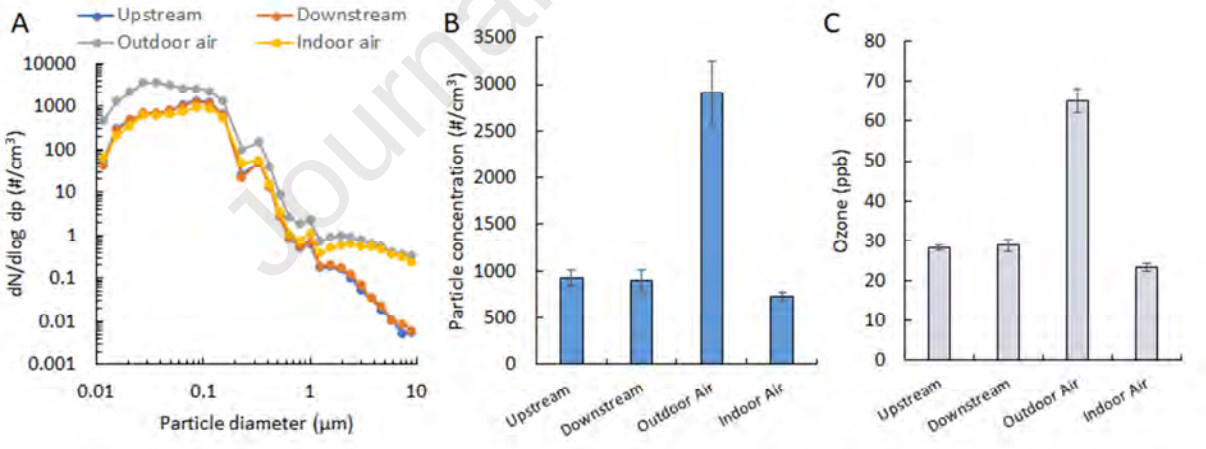

Figure 9. a) Particle size distributions, b) particle number concentrations, and c) ozone concentrations in an office building with operating needlepoint bipolar ionization (NPBI^{TM}) system. Upstream is the sampling location ~0.75 m upstream the ionizer in the supply air duct, while downstream is ~0.75 m downstream the ionizer in supply air duct. Note that both upstream and downstream sampling locations follow a MERV 8 filter, as described in Section 2.2 of the text.

In contrast with the particle and ozone measurements, Figure 10 shows that chemistry initiated by the ionizer appears to impact VOC concentrations within the duct (i.e., from upstream to downstream the ionizer unit). In particular, we observe increases in lower molecular weight,

Journal Pre-proof

oxygenated species which are expected to be reactive intermediates of the degradation processes initiated by the ionization unit. Ethanol, isopropanol, and acetone increased by approximately 133%, 213%, and 168% respectively, from upstream to downstream of the ionizer. As discussed previously, the ionization energies of these compounds indicate they should be ionized by the unit; net production of these compounds indicates they are also generated as a result of decomposition or rearrangement reactions. We also observed increases in heptane (230%) and methyl methacrylate (429%) and decreases in larger molecular weight fluorinated compounds. Interestingly, and consistent with the observations in the chamber studies, we observed an increase in toluene and a decrease in xylene levels downstream of the ionizer unit.

We also semi-quantified select aldehydes, acids, alcohols, and other compounds, shown aggregated in Figure 10, as we are less confident in quantification and identification than those compounds present in our calibration standard (explained in Appendix 3). Full reporting of compounds shown is shown in Appendix 4. Indoor concentrations of VOCs (labeled “Office”) are higher than downstream the ionizer, primarily due to substantial increases in ethanol, isopropanol, and acetone. These compounds may be generated in the space by ion-initiated chemistry, although they are also are emitted from humans (Pagonis et al., 2019; Tang et al., 2016) and other indoor sources (Wooley et al., 1990) such as hand sanitizers and other alcohol-based products. We are unable to discern the relative contribution of the ionizer-initiated chemistry vs. indoor sources to the observed the elevated indoor concentrations in this field study.

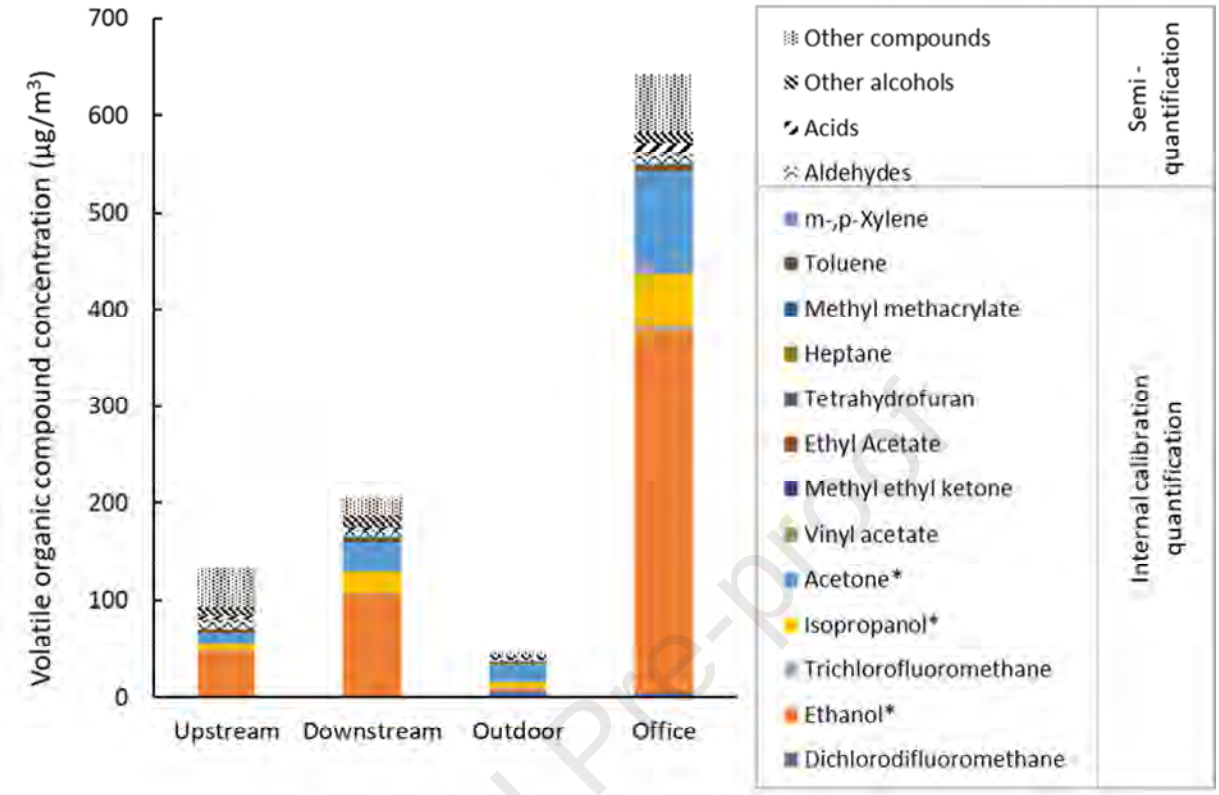

Figure 10. Summary of VOC monitoring in an occupied office building with an operating needlepoint bipolar ionization system. Upstream is the sampling location ~0.75 m upstream the ionizer in the supply air duct, while downstream is ~0.75 m downstream the ionizer in supply air duct. "*" denotes concentrations extrapolated from the calibration curve.

4. Discussion and Conclusions

Results from the chamber experiments conducted under normal operating conditions described herein suggest there were small reductions in inside/outside chamber ratios for three particle measures of total SMPS (~0.01-0.3 µm) number concentrations, total OPS (0.3-10 µm) number concentrations, and $PM_{2.5}$ mass concentrations, but the differences were not statistically significant and were partially impacted by simultaneous changes in the surrounding laboratory. Results from the particle injection and decay experiments in the same chamber suggest that the operation of the ionization unit in the test chamber appeared to have led to a slight increase in loss rates for ultrafine particles (<0.15 µm) and a slight decrease in loss rates for larger particles (>0.3 µm), resulting in a negligible net change in $PM_{2.5}$ loss rates. This observation is

conceivably explained by agglomeration of smaller particles that grew out of the <0.15 µm size range and appeared in the >0.3 µm size range but did not grow large enough to encourage more rapid deposition to surfaces in the test chamber. In other words, while these results suggest that the reported mechanism of action of the ionizer (agglomeration or particle growth) may be working, estimated particle mass was still conserved, and the ionizer function shifted the size distribution slightly in the direction of larger particles. Results from the field study revealed similar particle number and size distributions upstream and downstream of the ionization unit, suggesting there were minimal impacts in this short duct length in this installation (which occurred after a MERV 8 particle filter).

O_3 was not observed as a byproduct of operation of the tested device. The ionizer used in this study is designed to ionize molecules with ionization energies <12.07 eV (Waddell, 2019), which is below the ionization energy of molecular oxygen (O_2). This criterion is important, as ionizing O_2 is a key method for generating ozone (O_3), a known air pollutant, and, as mentioned, a common drawback to many ionizer devices in the past. This approach appears to successfully prevent O_3 formation as tested here.

Both the laboratory and field data collected herein suggest that other unintended byproduct formation (e.g., of smaller, potentially oxidized VOCs) is likely occurring, with some consistencies observed in both constituent reductions (e.g., xylenes, ethylbenzene, and 1,2-dichloroethane) and increases (e.g., acetone, ethanol, and toluene), with some consistencies observed between both the chamber tests and field tests. The concept behind ionization with respect to VOCs is that if the ionization energy is below that of the system, the VOCs will lose an electron and become positively charged ions, VOC+. These VOC+ ions could then be removed through electrostatic interactions with surfaces or to a negatively charged plate (if present). However, between initial ionization and removal, many chemical reactions can occur,

producing uncharged, neutral products that would no longer be easily removed. If the ionizer were able to sequentially ionize these neutral daughter products, then these products would not influence indoor air. However, if the residence time in the ionizing region is insufficient to fully ionize not only the parent VOCs initially in the indoor air, but also the multiple generations of daughter products, then the unintended consequence of ionizers may be to enhance concentrations of smaller, potentially oxidized daughter VOCs.

VOC+ ions formed in an ionizer have several possible fates in the indoor environment: they may (i) be removed to surfaces or (ii) react with neutral molecules in the gas phase to form an array of products. These ion-molecule reactions include adduct formation, charge transfer, and hydride transfer, and the mechanism of reaction determines the product and potential for formation of ultrafine particles versus oxygenated VOC or other products. Adduct formation, or clustering, can lead to new particle formation if additional molecules or ions continue to cluster to the initial adduct. Researchers have shown that ion-molecule reactions are central to new particle formation: clusters of ions and molecules rapidly grow to form small particles and are clearly correlated to particle growth events in the atmosphere (Kulmala et al., 2014).

This work is not without limitations and future directions for improvement. For one, this work was limited to a small number of field and laboratory experiments of a single bipolar ionization device, without replicates. For two, we relied on a limited set of analytical approaches, especially for gas-phase organics detection and quantification. Third, we did not evaluate efficacy for microbiological constituents, despite the high level of interest in these types of technologies for inactivating opportunistic pathogens such as SARS-CoV-2. Regardless of these limitations, this work highlights the need to improve and standardize methods of testing air cleaning technologies to capture the net effects of contaminant removal and/or generation on indoor air.

Given the rapid acceleration in the use of these types of electronic air cleaning technologies and many others, additional work should strive to expand and ultimately standardized test methods for evaluating the efficacy and potential for byproduct formation of these devices, especially those that rely on chemical interactions to remove or inactivate pollutants from air. Ionizer products in particular should be tested in greater quantity and variety, and under other realistic operating configurations (e.g., different ion concentrations, recirculating air configurations, non-well-mixed spaces with varying vertical or horizontal ion distributions). Further efficacy and byproduct testing should explore the impact of other indoor VOC challenge mixtures, including the impact of occupants, perhaps specific to building use types or occupancy scenarios. Test approaches should consider the use of a broader array of analytical approaches, such as additional organic analysis beyond the GC-MS and HPLC approaches and analyte lists used herein, including but not limited to real-time organics analysis, semi-volatile compounds, and especially inactivation of pathogens or surrogate organisms.

Journal Pre-proof

Acknowledgements

We would like to acknowledge Ian Cull for loaning sampling pumps for DNPH cartridges and a ppbRAE PID for real-time VOC detection, STAT Analysis for their analytical support, and several colleagues (who will remain anonymous) who provided their insight on experiences with installations of the tested ionizer and also loaned equipment for our testing.

This research did not receive any specific grant from funding agencies in the public, commercial, or not-for-profit sectors.

References

ASHRAE, 2020. Filtration/Disinfection. ASHRAE COVID-19 Resources. URL https://www.ashrae.org/technical-resources/filtration-disinfection

ASHRAE, 2018. ASHRAE Position Document on Filtration and Air Cleaning.

ASHRAE, 2017. Standard 52.2: Method of testing general ventilation air-cleaning devices for removal efficiency by particle size.

Bennett, D.H., Fisk, W., Apte, M.G., Wu, X., Trout, A., Faulkner, D., Sullivan, D., 2012. Ventilation, temperature, and HVAC characteristics in small and medium commercial buildings in California: Small and medium commercial buildings in California. Indoor Air 22, 309–320. https://doi.org/10.1111/j.1600-0668.2012.00767.x

BOMA, 2020. Getting Back to Work 2.0: Building Re-Entry: Best Practices in a COVID-19 Reality.

CDC, 2020a. Scientific Brief: SARS-CoV-2 and Potential Airborne Transmission. Coronavirus Disease 2019 (COVID-19). URL https://www.cdc.gov/coronavirus/2019-ncov/more/scientific-brief-sars-cov-2.html

CDC, 2020b. Coronavirus Disease 2019 (COVID-19): Community, Work & School - Ventilation. URL https://www.cdc.gov/coronavirus/2019-ncov/community/ventilation.html

Chan, W.R., Cohn, S., Sidheswaran, M., Sullivan, D.P., Fisk, W.J., 2015. Contaminant levels, source strengths, and ventilation rates in California retail stores. Indoor Air 25, 381–392. https://doi.org/10.1111/ina.12152

Cheng, Y.S., Bechtold, W.E., Yu, C.C., Hung, I.F., 1995. Incense Smoke: Characterization and Dynamics in Indoor Environments. Aerosol Science and Technology 23, 271–281. https://doi.org/10.1080/02786829508965312

Direct Supply, 2020. 11 Questions on a Proven Pathogen-Reducing Air Cleaning System. URL https://www.directsupply.com/blog/11-questions-on-a-proven-pathogen-reducing-air-cleaning-system/

Dong, W., Liu, S., Chu, M., Zhao, B., Yang, D., Chen, C., Miller, M.R., Loh, M., Xu, J., Chi, R., Yang, X., Guo, X., Deng, F., 2019. Different cardiorespiratory effects of indoor air pollution intervention with ionization air purifier: Findings from a randomized, double-blind crossover study among school children in Beijing. Environmental Pollution 254, 113054. https://doi.org/10.1016/j.envpol.2019.113054

Elejalde-Ruize, A., 2020. What will it take to make diners feel safe indoors? Nearly 60% feel uneasy eating inside, so restaurants try sterilizing UV wands, tabletop air purifiers as winter looms. Chicago Tribune.

Environmental and Modelling Group (EMG), 2020. Potential application of air cleaning devices and personal decontamination to manage transmission of COVID-19. Scientific Advisory Group for Emergencies (SAGE).

GPS, 2019. GPS-FC48-AC Product Data Sheet.

Hyun, J., Lee, S.-G., Hwang, J., 2017. Application of corona discharge-generated air ions for filtration of aerosolized virus and inactivation of filtered virus. Journal of Aerosol Science 107, 31–40. https://doi.org/10.1016/j.jaerosci.2017.02.004

ISO, 2016. ISO 16890: Air filters for general ventilation.

Ji, X., Le Bihan, O., Ramalho, O., Mandin, C., D'Anna, B., Martinon, L., Nicolas, M., Bard, D., Pairon, J.-C., 2010. Characterization of particles emitted by incense burning in an experimental house. Indoor Air 20, 147–158. https://doi.org/10.1111/j.1600-0668.2009.00634.x

Johnson Controls, 2020. 2020 Johnson Controls Energy Efficiency Indicator Study: COVID-19 Pulse Survey.

Kim, K.-H., Szulejko, J.E., Kumar, P., Kwon, E.E., Adelodun, A.A., Reddy, P.A.K., 2017. Air ionization as a control technology for off-gas emissions of volatile organic compounds.

Environmental Pollution 225, 729–743. https://doi.org/10.1016/j.envpol.2017.03.026
Kulmala, M., Petäjä, T., Ehn, M., Thornton, J., Sipilä, M., Worsnop, D.R., Kerminen, V.-M., 2014. Chemistry of atmospheric nucleation: on the recent advances on precursor characterization and atmospheric cluster composition in connection with atmospheric new particle formation. Annu Rev Phys Chem 65, 21–37. https://doi.org/10.1146/annurev-physchem-040412-110014
Liu, W., Huang, J., Lin, Y., Cai, C., Zhao, Y., Teng, Y., Mo, J., Xue, L., Liu, L., Xu, W., Guo, X., Zhang, Y., Zhang, J.J., 2020. Negative Ions Offset Cardiorespiratory Benefits of $PM_{2.5}$ Reduction from Residential Use of Negative Ion Air Purifiers. Indoor Air ina.12728. https://doi.org/10.1111/ina.12728
Mandavilli, A., 2020. How to Keep the Coronavirus at Bay Indoors. The New York Times.
Meschke, S., Smith, B.D., Yost, M., Miksch, R.R., Gefter, P., Gehlke, S., Halpin, H.A., 2009. The effect of surface charge, negative and bipolar ionization on the deposition of airborne bacteria. Journal of Applied Microbiology 106, 1133–1139. https://doi.org/10.1111/j.1365-2672.2008.04078.x
Nunayon, S.S., Zhang, H.H., Jin, X., Lai, A.CK., 2019. Experimental evaluation of positive and negative air ions disinfection efficacy under different ventilation duct conditions. Building and Environment 158, 295–301. https://doi.org/10.1016/j.buildenv.2019.05.027
Ori, R., 2020. Worries about COVID-19 spreading through the vents send Chicago building owners in search of cleaner air. 'You can't put a force field around your property.' Chicago Tribune.
Pagonis, D., Price, D.J., Algrim, L.B., Day, D.A., Handschy, A.V., Stark, H., Miller, S.L., de Gouw, J., Jimenez, J.L., Ziemann, P.J., 2019. Time-Resolved Measurements of Indoor Chemical Emissions, Deposition, and Reactions in a University Art Museum. Environ. Sci. Technol. 53, 4794–4802. https://doi.org/10.1021/acs.est.9b00276
Park, J.H., Yoon, K.Y., Hwang, J., 2011. Removal of submicron particles using a carbon fiber ionizer-assisted medium air filter in a heating, ventilation, and air-conditioning (HVAC) system. Building and Environment 46, 1699–1708. https://doi.org/10.1016/j.buildenv.2011.02.010
Patel, S., Sankhyan, S., Boedicker, E.K., DeCarlo, P.F., Farmer, D.K., Goldstein, A.H., Katz, E.F., Nazaroff, W.W., Tian, Y., Vanhanen, J., Vance, M.E., 2020. Indoor Particulate Matter during HOMEChem: Concentrations, Size Distributions, and Exposures. Environ. Sci. Technol. 54, 7107–7116. https://doi.org/10.1021/acs.est.0c00740
Perez, V., Alexander, D.D., Bailey, W.H., 2013. Air ions and mood outcomes: a review and meta-analysis. BMC Psychiatry 13, 29. https://doi.org/10.1186/1471-244X-13-29
Persily, A., Gorfain, J., 2004. Analysis of Ventilation Data from the U.S. Environmental Protection Agency Building Assessment Survey and Evaluation (BASE) Study (No. NISTIR 7145). National Institute of Standards and Technology (NIST).
Pushpawela, B., Jayaratne, R., Nguy, A., Morawska, L., 2017. Efficiency of ionizers in removing airborne particles in indoor environments. Journal of Electrostatics 90, 79–84. https://doi.org/10.1016/j.elstat.2017.10.002
Salonen, H., Salthammer, T., Morawska, L., 2019. Human exposure to NO2 in school and office indoor environments. Environment International 130, 104887. https://doi.org/10.1016/j.envint.2019.05.081
Shi, B., Ekberg, L., 2015. Ionizer Assisted Air Filtration for Collection of Submicron and Ultrafine Particles—Evaluation of Long-Term Performance and Influencing Factors. Environ. Sci. Technol. 49, 6891–6898. https://doi.org/10.1021/acs.est.5b00974
Tang, X., Misztal, P.K., Nazaroff, W.W., Goldstein, A.H., 2016. Volatile Organic Compound Emissions from Humans Indoors. Environ. Sci. Technol. 50, 12686–12694. https://doi.org/10.1021/acs.est.6b04415
US EPA, 2018. Residential Air Cleaners: A Technical Summary, 3rd edition.

US EPA, n.d. Summarized Data of the Building Assessment Survey and Evaluation Study. US EPA Indoor Air Quality. URL https://www.epa.gov/indoor-air-quality-iaq/summarized-data-building-assessment-survey-and-evaluation-study

Waddell, C., 2019. An Overview of Needlepoint Bipolar Ionization.

Wooley, J., Nazaroff, W., Hodgson, A., 1990. Release of Ethanol to the Atmosphere During Use of Consumer Cleaning Products. Journal of the Air & Waste Management Association 40, 1114–1120.

Wu, Y.-Y., Chen, Y.-C., Yu, K.-P., Chen, Y.-P., Shih, H.-C., 2015. Deposition Removal of Monodisperse and Polydisperse Submicron Particles by a Negative Air Ionizer. Aerosol Air Qual. Res. 15, 994–1007. https://doi.org/10.4209/aaqr.2014.08.0166

Xu, J., Jiang, H., Zhao, H., Stephens, B., 2017. Mobile Monitoring of Personal NOx Exposures during Scripted Daily Activities in Chicago, IL. Aerosol Air Qual. Res. 17, 1999–2009. https://doi.org/10.4209/aaqr.2017.02.0063

Xu, R., Yu, P., Abramson, M.J., Johnston, F.H., Samet, J.M., Bell, M.L., Haines, A., Ebi, K.L., Li, S., Guo, Y., 2020. Wildfires, Global Climate Change, and Human Health. N Engl J Med NEJMsr2028985. https://doi.org/10.1056/NEJMsr2028985

Yamada, M., Takaya, M., Ogura, I., 2015. Performance evaluation of newly developed portable aerosol sizers used for nanomaterial aerosol measurements. Industrial Health. https://doi.org/10.2486/indhealth.2014-0243

Zhang, Y., Mo, J., Li, Y., Sundell, J., Wargocki, P., Zhang, J., Little, J.C., Corsi, R., Deng, Q., Leung, M.H.K., Fang, L., Chen, W., Li, J., Sun, Y., 2011. Can commonly-used fan-driven air cleaning technologies improve indoor air quality? A literature review. Atmospheric Environment 45, 4329–4343. https://doi.org/10.1016/j.atmosenv.2011.05.041

Zhao, H., Gall, E.T., Stephens, B., 2019. Measuring the Building Envelope Penetration Factor for Ambient Nitrogen Oxides. Environ. Sci. Technol. 53, 9695–9704. https://doi.org/10.1021/acs.est.9b02920

Zhao, H., Stephens, B., 2017. Using portable particle sizing instrumentation to rapidly measure the penetration of fine and ultrafine particles in unoccupied residences. Indoor Air 27, 218–229. https://doi.org/10.1111/ina.12295

Zhao, H., Stephens, B., 2016. A method to measure the ozone penetration factor in residences under infiltration conditions: application in a multifamily apartment unit. Indoor Air 26, 571–581. https://doi.org/10.1111/ina.12228

Zhou, S., Young, C.J., VandenBoer, T.C., Kahan, T.F., 2019. Role of location, season, occupant activity, and chemistry in indoor ozone and nitrogen oxide mixing ratios. Environ. Sci.: Processes Impacts 21, 1374–1383. https://doi.org/10.1039/C9EM00129H

Journal Pre-proof

Journal Pre-proof

Supplementary Information (SI)
Contents Include:
Figures S1-S4
Appendix 1-4
Additional References

Chamber Mixing Investigation

A CO_2 injection and decay test was conducted to investigate mixing conditions in the test chamber with the air handling unit (AHU) operating. Four Extech SD800 CO_2 monitors, which were calibrated against each other using short-term co-location measurements, were placed in three different locations within the chamber (middle of the room on a desk, at the sampling location, and elevated in a corner on a ladder) and one location outside the chamber (near the AHU). CO_2 was briefly injected into the AHU from outside the chamber and each CO_2 monitor logged data at 5-second intervals. Figure S1a shows time-series CO_2 concentrations measured in the three monitoring locations before, during, and after CO_2 injection. The time-series data show good agreement between CO_2 measurements at each location, especially after the first ~15 minutes of CO_2 injection after allowing for mixing of the point source CO_2 entry. The mean CO_2 concentration measured during the subsequent decay period was 717 ppm in the central (desk) location, 707 ppm at the elevated (ladder) location, and 729 ppm at the primary instrument sampling location (i.e., a maximum relative difference in mean concentrations of ~3%). Figure S1b shows estimates of air change rates made at each of the three sampling locations inside the chamber using data from the CO_2 decay period. Air change rate estimates ranged from 1.57 per hour in the central (desk) location, 1.69 per hour at the elevated (ladder) location, and 1.67 per hour at the primary instrument sampling location (i.e., a maximum relative difference in of ~7%). Both measures of mixing confirm the chamber was operated at reasonably well-mixed conditions for the purposes of the tests conducted herein (i.e., <10% differences among chamber sampling locations for both of these metrics).

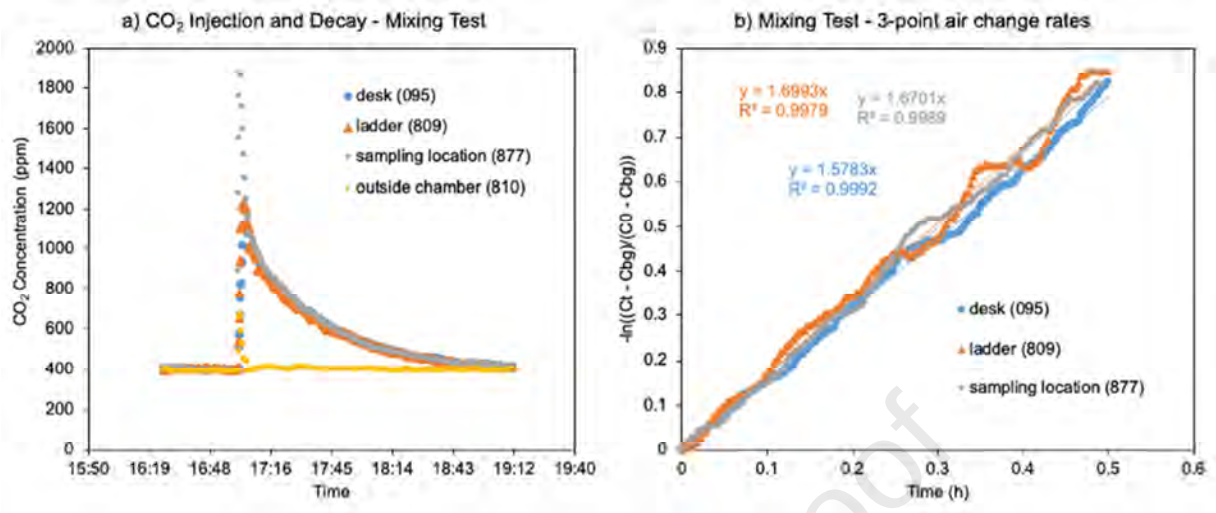

Figure S1. Chamber mixing tests: a) time-series CO_2 concentrations measured in three inside-chamber locations and outside the chamber before, during, after CO_2 injection and b) estimated air change rates in the three monitoring locations inside the chamber. The three-digit numbers next to each monitoring location corresponds to a portion of the serial number for each instrument.

Steady-State Conditions: TVOCs

Figure S2 shows time varying TVOC concentrations (as isobutylene equivalents) measured in the chamber as furniture and materials were brought in to create an indoor VOC mixture prior to testing.

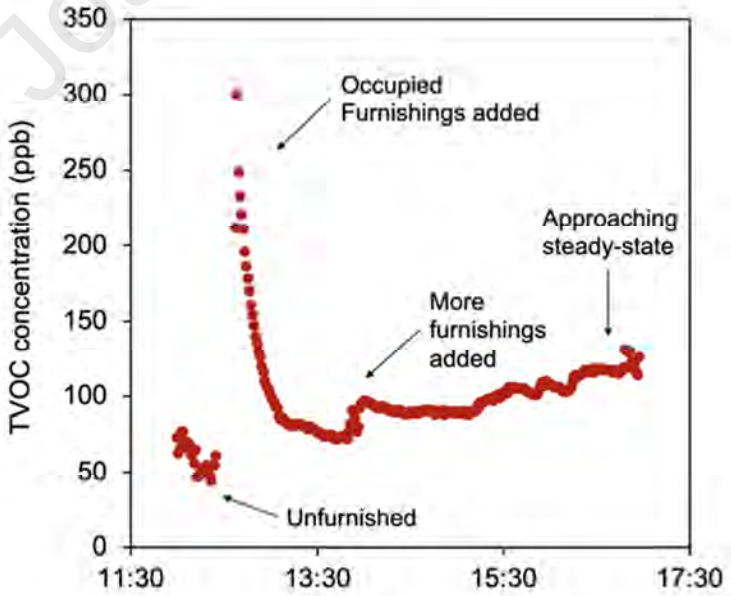

Figure S2. TVOC concentrations (as isobutylene equivalents) measured on October 9, 2020 as the chamber went from completely unfurnished to furnished and eventually approaching steady-state

Time-series O_3 Concentrations

Figure S3 shows time-series O_3 concentrations measured in the chamber during normal operating conditions.

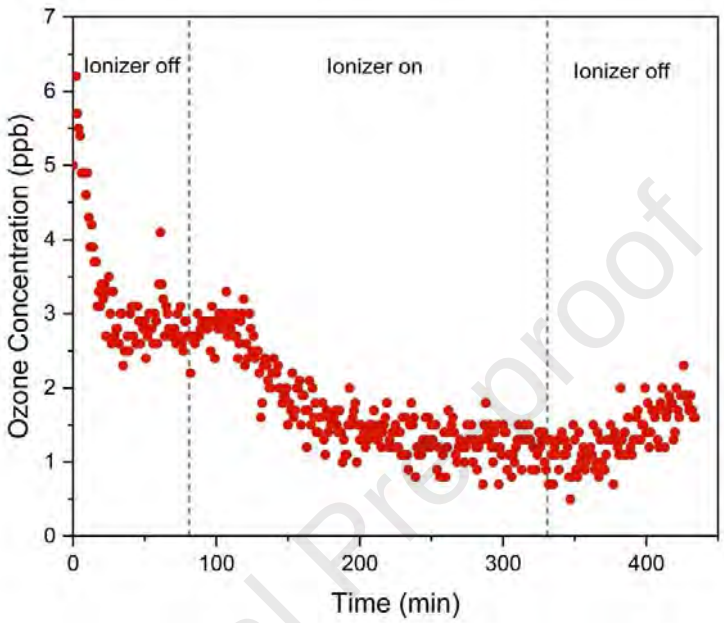

Figure S3. Time-resolved O_3 concentration in the chamber on one of the normal condition test days (October 24, 2020).

Journal Pre-proof

Air Change Rate Estimates during Particle Injection and Decay

Figure S4 shows results from air change rate measurements using CO_2 injection and decay made during the particle injection and decay experiments conducted on October 31, 2020 (with the ionizer on) and November 8, 2020 (with the ionizer off).

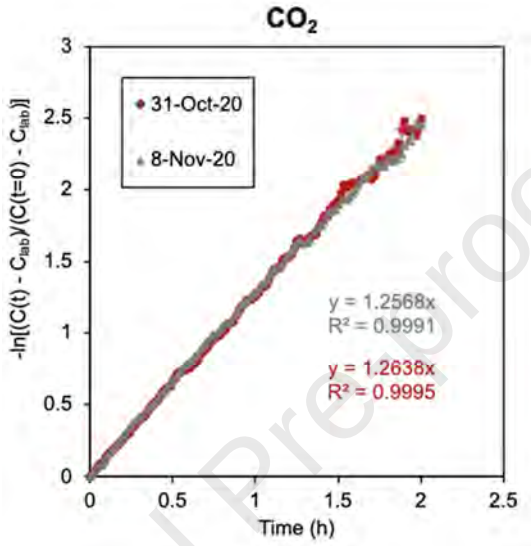

Figure S4. Air change rate estimates using CO_2 tracer injection and decay after particle injection and decay experiments were conducted on October 31, 2020 (ionizer test day) and November 8, 2020 (background, i.e., no ionizer, test day).

Journal Pre-proof

Appendix 1: List of TO-15 VOC analytes and reported concentrations from chamber tests

Test Method	Analyte	Units	Ionizer On		Ionizer Off	
			Inside	Outside	Inside	Outside
TO-15	1,1,1-Trichloroethane	mg/m³	< 0.0033	< 0.0033	< 0.0033	< 0.0033
TO-15	1,1,2-Trichloroethane	mg/m³	< 0.0033	< 0.0033	< 0.0033	< 0.0033
TO-15	1,1-Dichloroethane	mg/m³	< 0.0024	< 0.0024	< 0.0024	< 0.0024
TO-15	1,1-Dichloroethene	mg/m³	< 0.0024	< 0.0024	< 0.0024	< 0.0024
TO-15	1,2,4-Trichlorobenzene	mg/m³	< 0.0046	< 0.0046	< 0.0045	< 0.0045
TO-15	1,2-Dibromoethane	mg/m³	< 0.0046	< 0.0046	< 0.0045	< 0.0045
TO-15	1,2-Dichlorobenzene	mg/m³	< 0.0036	< 0.0037	< 0.0036	< 0.0036
TO-15	1,2-Dichloroethane	mg/m³	0.0041	< 0.0024	< 0.0024	< 0.0024
TO-15	1,2-Dichloropropane	mg/m³	< 0.0027	< 0.0027	< 0.0027	< 0.0027
TO-15	1,4-Dichlorobenzene	mg/m³	< 0.0036	< 0.0037	< 0.0036	< 0.0036
TO-15	1,4-Dioxane	mg/m³	< 0.0055	< 0.0055	< 0.0054	< 0.0055
TO-15	2-Butanone	mg/m³	< 0.0046	< 0.0046	< 0.0045	< 0.0045
TO-15	Acetone	mg/m³	0.023	0.036	0.041	0.037
TO-15	Benzene	mg/m³	< 0.0018	< 0.0018	< 0.0018	< 0.0018
TO-15	Bromodichloromethane	mg/m³	< 0.0039	< 0.0040	< 0.0039	< 0.0039
TO-15	Bromoform	mg/m³	< 0.016	< 0.016	< 0.016	< 0.016
TO-15	Bromomethane	mg/m³	< 0.0058	< 0.0058	< 0.0057	< 0.0058
TO-15	Carbon disulfide	mg/m³	< 0.0019	< 0.0019	< 0.0019	< 0.0019
TO-15	Carbon tetrachloride	mg/m³	< 0.0039	< 0.0040	< 0.0039	< 0.0039
TO-15	Chlorobenzene	mg/m³	< 0.0027	< 0.0027	< 0.0027	< 0.0027
TO-15	Chloroform	mg/m³	< 0.0030	< 0.0030	< 0.0030	< 0.0030
TO-15	cis-1,2-Dichloroethene	mg/m³	< 0.0024	< 0.0024	< 0.0024	< 0.0024
TO-15	cis-1,3-Dichloropropene	mg/m³	< 0.0027	< 0.0027	< 0.0027	< 0.0027
TO-15	Dibromochloromethane	mg/m³	< 0.0052	< 0.0052	< 0.0051	< 0.0052
TO-15	Dichlorodifluoromethane	mg/m³	0.0036	< 0.0030	< 0.0030	< 0.0030
TO-15	Ethylbenzene	mg/m³	0.0075	< 0.0027	< 0.0027	< 0.0027
TO-15	m,p-Xylene	mg/m³	0.024	< 0.0052	< 0.0051	< 0.0052
TO-15	Methyl tert-butyl ether	mg/m³	< 0.0021	< 0.0021	< 0.0021	< 0.0021
TO-15	Methylene chloride	mg/m³	< 0.021	< 0.021	< 0.021	< 0.021
TO-15	Naphthalene	mg/m³	< 0.0030	< 0.0030	< 0.0030	< 0.0030
TO-15	o-Xylene	mg/m³	< 0.0027	< 0.0027	< 0.0027	< 0.0027
TO-15	Styrene	mg/m³	< 0.0027	< 0.0027	< 0.0027	< 0.0027
TO-15	Tetrachloroethene	mg/m³	< 0.0042	< 0.0043	< 0.0042	< 0.0042
TO-15	Toluene	mg/m³	0.0026	0.0045	0.0034	0.0051
TO-15	trans-1,2-Dichloroethene	mg/m³	< 0.0024	< 0.0024	< 0.0024	< 0.0024
TO-15	trans-1,3-Dichloropropene	mg/m³	< 0.0027	< 0.0027	< 0.0027	< 0.0027
TO-15	Trichloroethene	mg/m³	< 0.0033	< 0.0033	< 0.0033	< 0.0033
TO-15	Trichlorofluoromethane	mg/m³	< 0.0033	< 0.0033	< 0.0033	< 0.0033
TO-15	Vinyl acetate	mg/m³	< 0.021	< 0.021	< 0.021	< 0.021
TO-15	Vinyl chloride	mg/m³	< 0.0015	< 0.0015	< 0.0015	< 0.0015
TO-15	Xylenes, Total	mg/m³	0.025	< 0.0079	< 0.0079	< 0.0079

Journal Pre-proof

Appendix 2: List of TO-11A analytes and reported concentrations from chamber tests

Test Method	Analyte	Units	Ionizer On		Ionizer Off	
			Inside	Outside	Inside	Outside
TO-11A	2,5-Dimethylbenzaldehyde	µg/m^3	< RL[1]	< RL	< RL	< RL
TO-11A	Acetaldehyde	µg/m^3	5.9	5.4	5.7	4.6
TO-11A	Acetone	µg/m^3	29.6	23.0	26.0	19.4
TO-11A	Acrolein	µg/m^3	< RL	< RL	< RL	< RL
TO-11A	Benzaldehyde	µg/m^3	< RL	< RL	< RL	< RL
TO-11A	Butyraldehyde	µg/m^3	2.1	2.0	2.2	1.6
TO-11A	Crotonaldehyde	µg/m^3	< RL	< RL	< RL	< RL
TO-11A	Formaldehyde	µg/m^3	11.4	5.9	10.6	5.3
TO-11A	Hexaldehyde	µg/m^3	< RL	< RL	< RL	< RL
TO-11A	Isovaleraldehyde	µg/m^3	< RL	< RL	< RL	< RL
TO-11A	m,p-Tolualdehyde	µg/m^3	< RL	< RL	< RL	< RL
TO-11A	o-Tolualdehyde	µg/m^3	< RL	< RL	< RL	< RL
TO-11A	Propionaldehyde	µg/m^3	< RL	< RL	< RL	< RL
TO-11A	Valeraldehyde	µg/m^3	< RL	< RL	< RL	< RL

[1] RL = Reporting limit

Journal Pre-proof

Journal Pre-proof

Appendix 3: Sampling and analysis protocol TD-GC/MS used at the field site

Sorbent tubes. VOCs were collected by glass sorbent tubes (Perkin Elmer) packed with 180 mg of Carbotrap B followed by 70 mg of Carboxen 1000 (Pankow et al, 1998) using a portable sampling pump (Universal PCXR8, SKC Inc., USA) to draw in the air. The sorbent tubes were conditioned prior to the sampling at 320°C for an hour using pre-cleaned N_2 gas at 100 mL/min. Each sorbent tube was then sealed with stainless steel Swagelok end caps that had been baked for 90 min at 100°C. The endcaps were fitted with PTFE ferrules. The sealed tubes were then stored in two clean Ziploc bags at -18°C in a freezer and kept cold during transportation using a cooler containing reusable ice packs. The sampling and the analysis of the sorbent tubes occurred within a few days after conditioning.

VOC sampling. The sampling was performed at a flow rate around 50 mL/min for 60 minutes with a total sample volume of 3 L for samples upstream and downstream of the ionization unit. The outdoor and indoor air samplings were performed at a flow rate around 50 mL/min for 30 minutes with a total sample volume of 1.5 L. The flow rate was measured for each sample using a primary standard air flow calibrator (Gilian, Gilibrator 2). After sampling, the sorbent tubes were capped and stored in two clean Ziploc bags and kept cold during transportation using a cooler containing reusable ice packs. Back to the laboratory, they were stored in the freezer at -18°C until analysis.

Calibration standards loading. A six-point calibration curve was achieved using a TO-15 gas mixture containing a representative mix of VOCs (65 components) at 1 ppmv in N_2 from Linde (Alpha, NJ, USA) certified to ± 5% accuracy. This mixture allows for the identification and quantification of compounds. Six calibration sorbent tubes were spiked with 0.16 – 6.2 mL of the gas mixture using a 50 mL/min flow of precleaned N_2 gas for 10 min. The spiked volume was withdrawn using a gastight syringe at atmospheric pressure and then injected into the sidearm of a Swagelok tee. The tee was connected to the N_2 flow on one side and to the inlet end of the sorbent tube on the other side (Pankow et al, 1998). The mass of compounds loaded into the standard sorbent tubes ranged from 0.3 to 71.7 ng (depending on the compounds). Standard sorbent tubes were analyzed following the same analysis method as for the samples, described below. Four internal standards were injected at a constant concentration in each sorbent tubes (including standards, samples and blanks): fluorobenzene, toluene-D8, bromofluorobenzene and 1,2-dichlorobenzene-D4. An internal standard normalized response ratio (e.g., compound area/internal standard area using the closest internal standard in terms of retention time) was then calculated and plotted against the theoretical mass loaded into the sorbent tube. The response of the analytical system was linear through the origin over this range.

Breakthrough test. Volume breakthrough tests have been performed at a mass spectrometry facility at Portland State University in the past, and showed that sample volume should not exceed 5 L using these sorbent tubes.

Sorbent tubes analysis. A total of 22 sorbent tubes including blanks were then analyzed using an Absorption/Thermal Desorption (ATD) instrument (TurboMatrix 650, PerkinElmer) connected

to a gas chromatograph (model 7890 A, Agilent Technologies) with a DB-VRX column (60 m length × 0.25 mm i.d. × 1.4 µm film thickness, Agilent J&W) coupled to a mass selective detector (model 5975 C, Agilent Technologies). The ATD instrument desorbed each sorbent tube at 300 °C during 10 min, and samples were then concentrated into a cold trap at -30 °C after which they were injected in a split/splitless injector kept at 180 °C. The injector was in split mode with a split flow of 2.76 $mL.min^{-1}$. Helium was used as the carrier gas at a constant flow of 0.92 $mL.min^{-1}$. The oven temperature started at 45 °C for 10 min, was then raised at 12 $°C.min^{-1}$ up to 190 °C and kept isothermal for 2 min, then raised again at 6 $°C.min^{-1}$ up to 240 °C and kept isothermal for 1 min and finally decreased at 10 $°C.min^{-1}$ to 210 °C. The MS conditions were: transfer line at 230 °C, ion source at 250 °C and EI voltage at 70 eV. Data were recorded in full scan mode (*m/z* range: 34-400 amu). Peaks integration was performed using Agilent ChemStation software. Compounds were identified on the basis of their mass spectra and the injection of standards when available. The mass spectra were compared with those from two databases: NIST Mass Spectral Database (2008) (NIST08) and W8N08 library (John Wiley & Sons, Inc., USA). Peak integration was based on extracted ion chromatograms (quantifier ions). Moreover, four internal standards were injected in each sample in order to i) use the internal standard normalized response factor to calculate the concentration of target compounds, ii) check the method (desorption and analysis) efficiency, evaluate the instrument and method performance, iii) get a relative concentration for the compounds for which we do not have standards. 98 compounds were extracted from the mass spectra for identified peaks with a signal/noise ratio of > 3 standard deviations. 40 compounds were above the quantification threshold (signal/noise ratio of > 10 standard deviations and within the external calibration range).

Quantification

Compounds included in the TO-15 mixture: Compounds mass on each sorbent tube was calculated by imputing the compound internal standard normalized area into the linear fit line equation from the corresponding calibration curve. Concentrations were then calculated by dividing mass by sampling volume for each sorbent tube.

Compounds not included in the TO-15 mixture: Semi-quantification was estimated using the response factor determined for the nearest compounds in the TO-15 mixture in terms of retention time. The response factor (RF) is calculated using the following equation:

$RF = ((A_X)\times(C_{ISTD}))/((A_{ISTD})\times(C_X))$

Where A_X is the area of the nearest compound, C_X the concentration of the nearest compound, A_{ISTD} is the area of the internal standard, C_{ISTD} is the concentration of the internal standard. The response factor is calculated for each level of the calibration and an averaged response factor is then calculated (RF_{AVE}). The following equation is then used to calculate the concentration of the target compound:

$C_X = [((A_X)\times(C_{ISTD}))/((A_{ISTD})\times(RF_{AVE}))]/\text{sample volume}$

QA/QC. A field blank was prepared and consisted in handling the sorbent tube the same way we do with the sample: take the sorbent tube from the Ziploc bag from the cooler bag, remove the end cap, plug the sorbent tube onto the pump, tight the fittings, prepare the pump, unplug the sorbent tube from the pump, cap the tube and place it in a new Ziploc bag into the cooler. A

transportation blank was analyzed consisting in a sorbent tube never uncapped until analysis and that was transported in the same way as other sorbent tubes. A storage blank was also analyzed consisting in a sorbent tube placed into the freezer after conditioning and analyzed at the same time as the other sorbent tubes. The transportation and storage blanks showed no contamination compared to freshly conditioned sorbent tubes.

References

Pankow et al, 1998: Pankow, J. F.; Luo, W.; Isabelle, L. M.; Bender, D. A.; Baker, R. J. Determination of a Wide Range of Volatile Organic Compounds in Ambient Air Using Multisorbent Adsorption/Thermal Desorption and Gas Chromatography/Mass Spectrometry. Anal. Chem. 1998, 70 (24), 5213–5221. https://doi.org/10.1021/ac980481t.

Journal Pre-proof

Appendix 4: Summary of compounds identified and quantified in the field site sampling (occupied office environment) by TD-GC-MS (μg/m^3)

Compounds	Calibration[1]	Upstream	Downstream	Outdoor	Office
Dichlorodifluoromethane	internal	2.12	1.52	4.69	4.23
Ethanol*	internal	44.96	104.97	3.06	372.95
Trichlorofluoromethane	internal	0.56	0.32	1.83	5.52
Isopropanol*	internal	7.32	22.89	5.37	53.99
Acetone*	internal	11.31	30.35	18.37	103.75
Vinyl acetate	internal	0.00	0.00	1.07	1.39
Methyl ethyl ketone	internal	0.65	0.66	0.19	1.00
Ethyl Acetate	internal	2.02	2.18	0.35	3.02
Tetrahydrofuran	internal	0.16	0.19	0.00	0.00
Heptane	internal	0.17	0.55	0.00	0.87
Methyl methacrylate	internal	0.09	0.45	0.28	0.54
Toluene	internal	1.12	1.28	0.86	1.33
m-,p-Xylene	internal	0.75	0.65	0.35	0.98
Aldehydes					
Acetaldehyde	semi-quant	1.03	0.99	0.00	4.27
n-Hexanal	semi-quant	0.77	0.27	0.00	0.49
Furfural	semi-quant	3.29	2.19	0.17	1.37
Benzaldehyde	semi-quant	0.61	0.59	0.18	1.65
Nonanal	semi-quant	1.88	1.24	0.84	1.55
Decanal	semi-quant	1.57	0.97	0.54	1.53
Total aldehydes		**9.15**	**6.25**	**1.73**	**10.86**
Acids					
Formic acid	semi-quant	0.00	1.18	0.00	0.00
Acetic acid	semi-quant	1.39	0.54	2.72	10.61
2-Methylpropanoic acid	semi-quant	0.14	0.23	0.00	0.00
Butanoic acid	semi-quant	2.06	1.11	0.00	0.48
Hexanoic acid	semi-quant	0.37	0.27	0.00	0.05
Total acids		**3.96**	**3.33**	**2.72**	**11.14**
Other alcohols					
1-Propanol	semi-quant	0.07	0.20	0.00	0.25
2-Methyl-3-buten-2-ol	semi-quant	0.73	0.97	0.31	0.87
1-Butanol	semi-quant	5.07	4.65	0.00	6.68
1-Methoxy-2-propanol	semi-quant	0.00	2.17	0.00	0.00
1-Pentanol	semi-quant	0.06	0.12	0.00	0.00
Phenol	semi-quant	1.03	0.97	0.46	0.70
2-Ethylhexanol	semi-quant	2.21	1.11	0.22	2.44
Total other alcohols		**9.18**	**10.19**	**0.98**	**10.94**
Other compounds					
Decamethylcyclopentasiloxane	semi-quant	31.45	13.97	0.84	51.95
Butyrolactone	semi-quant	0.00	0.40	0.00	0.00
Acetophenone	semi-quant	0.94	0.47	0.19	0.36
α-Pinene	semi-quant	0.63	0.34	0.08	0.37
Limonene	semi-quant	4.26	1.80	0.25	1.24
2-Methylhexane	semi-quant	0.38	0.41	0.00	0.53
Methylcyclohexane	semi-quant	0.36	0.44	0.00	0.66
1-Methoxy-2-propyl acetate	semi-quant	0.00	0.33	0.00	0.00
2-Methylbutane	semi-quant	1.90	1.50	3.94	4.08
Total other		**39.92**	**19.67**	**5.29**	**59.19**

[1]Internal = quantified using standard calibration (TO-15 mixture); Semi-quant = quantified using response factor calculated using internal standard and nearest compounds in the TO-15 standard

Journal Pre-proof

Highlights

- Laboratory and field tests conducted to characterize bipolar ionization device
- Evaluated impacts on gas and particle removal and byproduct formation
- Ionization decreased some hydrocarbons but increased others
- Ionization minimally impacted particles, ozone, and nitrogen dioxide
- Ionization shifted particle size distribution but did not impact $PM_{2.5}$ mass

Journal Pre-proof

Journal Pre-proof

Declaration of interests

☒ The authors declare that they have no known competing financial interests or personal relationships that could have appeared to influence the work reported in this paper.

☐The authors declare the following financial interests/personal relationships which may be considered as potential competing interests:

Journal Pre-proof